



WICHITA STATE
UNIVERSITY

UNIVERSITY LIBRARIES

Biomechanical effects of ankle sprain orthoses

Item Type	Thesis
Authors	Figueroa Reymundo, Pedro
Publisher	Wichita State University
Rights	Copyright 2017 by Pedro Figueroa All Rights Reserved
Download date	2026-05-13 09:39:45
Link to Item	http://hdl.handle.net/10057/15305

BIOMECHANICAL EFFECTS OF ANKLE SPRAIN ORTHOSES

A Thesis by

Pedro Figueroa Reymundo

Bachelor of Science, Wichita State University, 2013

Submitted to the Department of Mechanical Engineering
and the faculty of the Graduate School of
Wichita State University
in partial fulfillment of
the requirements for the degree of
Master of Science

December 2017

© Copyright 2017 by Pedro Figueroa

All Rights Reserved

BIOMECHANICAL EFFECTS OF ANKLE SPRAIN ORTHOSES

The following faculty members have examined the final copy of this thesis for form and content, and recommend that it be accepted in partial fulfillment of the requirement for the degree of Master of Science, with a major in Mechanical Engineering.

Hamid Lankarani, Committee Chair

Nils Hakansson, Committee Co-Chair

Yimesker Yihun, Committee Co-Chair

DEDICATION

A mis padres, quienes a lo largo de mi vida
se han preocupado por mi bienestar y educación
siendo mi apoyo en todo momento

Con mucho cariño les dedico todo mi esfuerzo
y trabajo puesto para la realización de esta tesis

ACKNOWLEDGEMENTS

I would like to express my best regards and sincere gratitude to my research advisors Dr. Hamid Lankarani, Dr. Nils Hakansson, and Dr. Yimesker Yihun. Their guidance, encouragement, knowledge and support made this work possible. I truly appreciate my friends Richard Sack and Rahul Agrawal for their guidance and support with all the technical issues and troubleshooting of the lab equipment. I would also like to thank my family members and friends for their support. Thank you to my cousins Adrian and Jose for helping me with pilot studies and preparing the equipment. Likewise, I want to show my gratitude to Matt Friling, Aaron Hodson, and William Marsh for their kind assistance in spite of their busy school schedule. Special thanks goes to the helpful and generous staff at Peeples Prosthetics for facilitating the ankle foot orthosis. This research would not have been possible without the research subjects. Thank you all for your participation.

ABSTRACT

When treating grade III ankle sprains, patients are often instructed to immobilize the affected ligaments in order to allow reparative healing. However, signs of functional instability are apparent after long periods of immobilization. Several studies have compared the efficacy of controlled range of motion walker boots and braces against traditional casts in reducing muscle activity. Nevertheless, the integrity of the affected ligaments during conservative and functional treatments of ankle sprains is a subject that is not yet fully understood. The main objective of this thesis is to use musculoskeletal dynamic simulations to study the effectiveness of functional articulated ankle foot orthoses in providing muscle stimulation, while simultaneously protecting the affected ligaments and accelerate recovery. Ligaments are passive structures that connect articulating bones and keep joints assembled. Mechanically they are much like muscles but with no active contractile element. To validate the simulated ligament forces, a comparison of EMG muscle activity is made against simulated muscle activity. Special attention is given to the tibialis anterior (TA), the extensor digitorum longus (EDL), and the peroneus longus (PL). Three walking conditions are introduced: regular walking (no ankle boot orthosis), walking with a rigid boot, and walking with an articulated boot. The experiments show that there is a significant difference between collected and simulated muscle activity of the PL. On the other hand, there is no overall significant difference between all walking conditions when comparing EMG activity and simulated activity of the TA and EDL muscles. Additionally, there is little change in ATFL ligament force loads between rigid and articulated orthoses. The research performed in this study indicates that the use of articulated ankle foot orthoses does in fact stimulate important muscle activity necessary for proper motor control while in turn maintaining the ATFL forces at a minimal. This conveys evidence that functional treatment should be preferred over conservative immobilization.

TABLE OF CONTENTS

Chapter	Page
1 INTRODUCTION.....	1
1.1 Motivation.....	2
1.2 Quick Statistics.....	3
1.3 Hypotheses/Objectives.....	4
1.4 Approach.....	4
1.5 Contribution.....	5
1.6 Outline (Structure and Organization).....	5
 2 LITERATURE STUDY.....	 6
2.1 Orthoses.....	6
2.1.1 History of Foot Orthoses.....	6
2.2.2 Ankle Foot Orthoses.....	8
2.2 Anatomy of the Human Foot.....	9
2.2.1 Biomechanics of the foot and Ankle.....	9
2.2.2 Dynamic support structures of the ankle junction.....	14
2.2.3 Mechanisms of ankle sprains.....	16
2.3 Human Gait Cycle.....	18
2.3.1 Definitions.....	18
2.3.2 Gait Phases.....	20
2.3.3 Analysis of Gait.....	24
2.3.4 Kinematics of Gait.....	24
2.3.5 Kinetics of Gait.....	25
2.3.6 Electromyography.....	25
2.4 Critical Review of Topics Pertaining Gait with Foot Orthoses.....	26
2.4.1 AFO Ground Reaction Forces (Kinetics and Kinematics).....	26
2.4.2 Work/Energy expenditure and use of electromyography with AFOs.....	34
2.4.3 Conclusion and Research Proposal.....	41
 3 METHODS.....	 42
3.1 Subjects.....	42
3.2 Experimental Protocols.....	42
3.3 Equipment.....	43
3.4 Modeling and Simulation.....	45
3.5 Method to Define the Beginning and End of Gait.....	48
3.6 Data Analysis.....	48
3.6.1 Anterior Talofibular Ligament Forces.....	48
3.6.2 Muscle Activity.....	48

TABLE OF CONTENTS (continued)

Chapter	Page
4 RESULTS AND DISCUSSION	50
4.1 Anterior Talofibular Ligament Forces	50
4.2 Muscle Activity	51
4.3 Discussion	54
4.4 Methodological Issues	55
4.5 Interpretation of Results	56
5 CONCLUSIONS AND RECOMMENDATIONS	62
5.1 Conclusions	62
5.2 Recommendations for Future Studies	63
REFERENCES	64
APPENDIXES	72
A Modified Gait Cycle	73
B Anterior Talofibular Ligament Forces and Ankle Joint Angles	74
C Average Simulated Muscle Activations from Computed Muscle Control and Average Experimental EMG	79
D Statistical Analyses	82
E Matlab Routine for Data Normalization	85
F Opensim Ligament Class	90

LIST OF TABLES

Table	Page
2.1 Mean Peak Vertical GRFs and Time to Peaks Mean (SD).....	32
4.1 Anterior Talofibular Ligament Peak Force.....	50
4.2 EMG Muscle Activity (Volts)	52
4.3 OpenSim Muscle Activity (Volts)	52

LIST OF FIGURES

Figure	Page
2.1 Talocrural joint (indicated by red demarcation).	10
2.2 Range of motion of the TCJ.....	11
2.3 Subtalar joint (indicated by red demarcation).....	11
2.4 Range of motion of the STJ	12
2.5 Lateral oblique view of ankle joint	13
2.6 Peroneus Longus and Brevis.....	15
2.7 Tibialis anterior.....	16
2.8 Mechanisms of a lateral ankle sprain and injury of ATFL	17
2.9 Mechanisms of a syndesmotic sprain. Injury of anterior tibiofibular ligament.....	18
2.10 Anatomical Planes.	19
2.11 Stride vs Step.	19
2.12 Plantar-flexion and dorsi-flexion.	20
2.13 Divisions of the gait cycle.....	20
2.14 Weight Acceptance	21
2.15 Mid stance, terminal stance, and pre-swing phase.....	23
2.16 Reflective markers placement on lower extremity and pelvis.....	28
2.17 Ground reaction forces and joint moments.....	29
2.18 Two short-leg walkers used in the study: gait walker (A) and equalizer (B)	31
2.19 Mean minimum GRFs, mean peak braking force, & mean peak propulsion force	33
2.20 EMG activity of 3 conditions as percent of barefoot activity.....	36

LIST OF FIGURES (continued)

Figure	Page
2.21 Insertion of cannula in tendon.....	38
2.22 Achilles tendon mean force curve and EMG activity.....	39
2.23 Achilles tendon mean force and mean rate.	39
2.24 Mean EMG activity of the soleus, gastrocnemius, and tibialis anterior muscles at a ± 95 confidence.....	40
3.1 Biomechanics lab.....	43
3.2 Markerset and virtual markers.	44
3.3 ENG detection system.....	44
3.4 OpenSim lumped torso/lower limbs model.	46
3.5 Talofibular ligament in OpenSim.	47
3.6 CMC simulation examples.....	49
4.1 Mean right tibialis anterior activity.....	53
4.2 Mean right extensor digitorum longus activity.	53
4.3 Mean right peroneus longus activity.....	53
5.1 Subject 2 ATFL forces vs ankle joint angles.	57
5.2 Subject 2 CMC no boot condition simulation.....	58
5.3 Subject 2 CMC articulated boot condition simulation.....	59
5.4 Subject 2 marker placement on boot.....	59

LIST OF ABBREVIATIONS

AFO	Ankle Foot Orthosis
AITFL	Anterior Tibiofibular Ligament
ANOVA	Analysis of Variance
ATF	Ankle Tendon Force
ATFL	Anterior Talofibular Ligament
CAM	Controlled Ankle Motion
CFL	Calcaneofibular Ligament
CI	Confidence Interval
CMC	Computed Muscle Control
CROM	Controlled Range of Motion
DF/pf	Dorsi-Flexion
EDL	Extensor Digitorum Longus
EMG	Electromyography
FI	Functional Instability
GRF	Ground Reaction Force
IC	Initial Contact
LSD	Least Significance Difference
PCSA	Physiological Cross Sectional Area
PF/pf	Plantar-Flexion
PITFL	Posterior Inferior Tibiofibular Ligament
PL	Peroneus Longus
PLS	Posterior Leaf Spring Orthosis

LIST OF ABBREVIATIONS (continued)

SD Standard Deviation

STJ Subtalar Joint

STJ Subtalar Joint

TA Tibialis Anterior

TCJ Talocrural Joint

CHAPTER ONE

INTRODUCTION

Ankle foot orthoses or AFOs are orthotic devices created to support and re-align the ankle complex and provide restriction or enforcement of motion. The use of these devices can lead to a reduction in symptoms, improvement of function, and a quick injury recovery [1]. Ankle sprain—particularly ankle inversion—is one of the most common musculoskeletal injuries. During such injuries, the lateral compartment of the ankle may suffer from grade I microscopic tearing, grade II partial tearing with ligamentous integrity, and in worst cases grade III complete tearing of ligaments[1] , [3] The use of an AFO for the treatment of an ankle sprain is crucial to properly immobilize the area and allow reparative healing of the affected ligaments. However, immobilization of an acute ankle sprain remains controversial. Usually, issues of immobilization come into question in the treatment of sprains that involve complete disruption of the ligaments otherwise known as a grade III rupture [4]. Additionally, a study that compared immobilization against functional treatment led to the conclusions that immobilization, if necessary, should be used only for short periods of time, and should otherwise be abandoned as treatment of choice for uncomplicated lateral ankle ligament injuries such as grade I and grade II [5] Controlled range of motion (CROM) walkers or articulated walkers are functional treatment AFOs which allow certain degrees of dorsiflexion and plantarflexion and are used in an effort to accelerate recovery through muscle stimulation while still treating and protecting the affected mediolateral ligaments [6]. Functional rehabilitation not only results in quicker recovery, but also helps to reduce residual complications that often occur after an ankle sprain [7]. During ankle sprains, mechanoreceptors and proprioceptive nerve endings get damaged creating functional instability (FI) making the individual susceptible to recurring ankle sprains with slight to no provocation whatsoever [8]. This

is because in terms of motor control, the human nervous system does not adequately locate the position of the leg and foot with respect to the floor. As a result, dorsiflexor muscles as well as peroneal musculature start to compensate for muscular paresis by minimizing plantarflexion and inversion. Studies show that people with FI exhibit evidence of a corrective mechanism occurring due to contraction of the peroneal muscles if the ankle joint inversion is perceived to be too great during the midswing to terminal swing phase of gait [9]. Similarly, another group of authors also noted an increase of peroneal muscle activity in subjects with FI. They realized that subjects would contact the ground during walking, and it was this sensory experience of contacting the ground that triggered a protective feed-forward mechanism in order to prevent future ankle sprains [8]. Current technologies for rehabilitation rely on a professional's qualitative judgment and trial-and-error to find the appropriate treatment for an ankle sprain. Literature seems to agree that concerning effectiveness, functional treatment currently seems a more appropriate treatment and should be encouraged [5]. The research in this study seeks to examine the appropriateness of the functional treatment approach with regards to inversion ankle sprains.

1.1 Motivation

In clinical practice, the question often arises whether an orthosis diminishes muscle activity, thereby worsening an existing paresis. An inevitable side effect of ankle/foot immobilization is the development of atrophy in the adjacent musculature as a result of increased periods of inactivity during motion restriction. Several studies have analyzed the effects of rigid and functional articulated AFOs on muscle activity and have highlighted that significant decrease of dorsiflexor musculature exists as a result of wearing a rigid AFO [10]. Some of these studies also obtained lower activity of peroneus longus. Literature indicates that injury to joint mechanoreceptors may occur during an ankle sprain, resulting in proprioceptive deficits and poor

ankle/foot biomechanics [11]. Reduced mechanical strength of the ligaments and proprioceptive deficits lead to joint laxity and impaired dynamic support of the surrounding musculature [12], [13]. To date, no study has used musculoskeletal dynamic simulations to corroborate the efficacy of a functional articulated AFO in promoting protective feed-forward muscle activation and replicating muscle activity typically found on non-pathological or regular gait patterns while at the same time protecting the affected ligaments. Through the use of musculoskeletal modeling and dynamic simulations it is possible to compare the effects that rigid and articulated AFOs have on muscle activity due to immobilization. This can shed light on the importance of functional rehabilitation and its role in stimulating sprain-preventive muscle reflexes that improve foot and ankle control for proper biomechanical function.

1.2 Quick Statistics

An estimated two million acute ankle sprains occur each year in the United States alone, resulting in aggregate health-care cost of \$2 billion [14]. This injury can result in considerable time lost to injury and long-term disability in up to 60% of patients. Ankle sprain is the most common injury in the athletic populations, accounting for up to 30% of sports injuries [14]. As for the different types of sprains, lateral or inversion ankle sprain is the most commonly observed. In one particular sports medicine clinic in the US, approximately 85% of ankle sprains presented were due to inversion [15]. In a study that compared ankle injuries suffered by national teams, competitive athletes and recreational athletes as much as 73% of all athletes had recurrent ankle sprains and 59% of these athletes had significant disability and residual symptoms of ankle pain, crepitus, instability and/or weakness [16].

1.3 Hypotheses/Objectives

In view of the previously mentioned studies, the following two-piece hypothesis is posed to guide the efforts of this research.

The difference in ligament forces between rigid and articulated walkers is negligible. Nevertheless, articulated AFOs permit dorsiflexion and plantarflexion allowing for a more normalized gait which in turn promotes functional ankle stability and stimulates proprioception. Specifically, it was hypothesized that:

- a. There is little change in the force loads on the Anterior Talofibular Ligament (ATFL)—the weakest of the lateral collateral ligaments—when walking with a rigid or articulated AFO.
- b. As opposed to wearing a rigid AFO, wearing an articulated AFO will enable protective feed-forward activation of the tibialis anterior (TA), the extensor digitorum longus (EDL) and the peroneus longus (PL). The TA and EDL are in charge of dorsiflexion while the PL controls eversion and plantarflexion. These movements are necessary for proper motor control, stability, and ground clearance to avoid recurring inversion sprains.

1.4 Approach

To test these hypotheses:

- Subjects were recruited,
- Kinetic, Kinematic, and EMG data were recorded for 3 scenarios (No-AFO, Rigid AFO, Articulated AFO),
- Computer simulations of the movements were generated, and the simulation outputs were compared to experimental data for validation and analyzed to assess ATFL loads.

1.5 Contribution

This thesis hopes to provide new insights in regards to early progressive rehabilitation by supporting functional treatment and its favorable outcome in protecting affected ligaments that have gone through trauma during ankle sprains.

1.6 Outline (Structure and Organization)

Chapter 1 introduces the reader to ankle foot orthoses, ankle sprains, and provides a quick overview of studies concerning functional treatment of ankle sprains. This chapter also explains the how the integrity of the affected ligaments during conservative and functional treatments of ankle sprains is a subject that is not yet fully understood. As a result, a hypothesis is proposed to provide guidance to the study. The approach used to perform the investigation is presented and the contribution of the research is shared. Chapter 2 presents a comprehensive collection of literature review concerning orthoses and their history, the anatomy of the human foot, the human gait cycle, and a series of topics pertaining gait in conjunction with an AFO. In chapter 3, the methodologies of the research are described in regards to the recruitment of subjects, experimental protocols, equipment, modeling and simulation development, and data analysis. The results are displayed in chapter 4 in two separate sections that link to the hypotheses posed. The first section shows the results of the ATFL while the results of the muscle activity are presented in the second section. Chapter 4 also presents discussion of such results by evaluating potential methodological issues and subsequently interpreting the results. Chapter 5 concludes the study followed by the references and appendices.

CHAPTER TWO

LITERATURE STUDY

This chapter presents the anatomy of the foot in terms of bones, joints, intrinsic muscles and ligaments, providing an overview of the important anatomical structures that need to be addressed to understand lateral ankle sprains. Additionally, the different human gait cycles are explained. Finally, a literature review pertaining existing studies of AFOs is covered. This includes ground reaction forces (kinetics, kinematics), and work/energy expenditure with AFOs.

2.1 Orthoses

2.1.1 History of Foot Orthoses

Biomechanics and foot orthoses have evolved over the centuries. Many talented individuals have increased our knowledge in foot and lower extremity biomechanics as well as foot orthoses. One of the early biomechanics authors was Aristotle. He provided some of the first scientific analysis of gait and first geometric analysis of muscular actions on bones in his treatise “De Motu Animalium (About the Movement of Animals)”[17]. He accurately described ground reaction force (GRF) when he said “Just as the pusher pushes, so the pushed is pushed, i.e. with similar force” [17]. The curiosity and desire to learn more about biomechanics provoked others to research human movement. In (129-201 AD) Galen, considered the first “sports physician” was a Roman physician and surgeon who first explained the difference between motor and sensory nerves as well as agonist and antagonist muscles in his work “De Motu Musculorum (On the Motion of Muscles)” [18]. In the high renaissance period Leonardo DaVinci, Italian painter, sculptor, and inventor made some of the first observations in human running: “He who runs down a slope has his axis on his heels; and he who runs uphill has it on the toes of his feet; and a man running on level ground has it first on his heels and then on the toes of his feet” [19]. The term “orthopedics”

meaning “straight child” was first coined in the eighteenth century by a French physician called Nicolas Andry. Andry stated, “If the feet incline too much to one side, you must give the child shoes that are higher on that side, both in the sole and heel, which will make him incline to the opposite side.” [20]. In the 19th century, Lewis Durlacher and other physicians and boot fabricators of his era were some of the first to use engineered leather devices for treatment of painful pathologies and deformities within the foot and lower extremity. Nevertheless, during the majority of the 19th century, medical doctors showed minor interest in treating foot problems. In 1895, a group of dedicated practitioners in New York successfully appealed to NY State Legislature to first establish “chiropody” (now known as podiatry) as a licensed profession [21]. Even though foot orthoses were being used by select medical practitioners in the first half of the 20th century, it was not until 1958 that the era of modern foot orthosis therapy began. In 1954, Merton Root—a California podiatrist—fabricated thermoplastic foot orthoses made around feet casted in a subtalar joint (STJ) rotational position also known as the neutral position. It was around this time when the era of modern prescription foot orthoses was born [22]. Foot orthoses have been utilized for hundreds of years to treat several pathologies and injuries in the medical profession. These orthoses have evolved from leather to cork and on to complex metallic structures projected to serve in therapeutic and rehabilitation procedures. The main functions of these orthoses are to treat painful pathologies and to prevent new injuries of the foot and lower extremities. Additionally, other applications deal with the optimization of the biomechanics of the individual during sports and other weight-bearing activities.

2.2.2 Ankle Foot Orthoses

Solid Ankle Foot Orthoses

The most prescribed ankle foot orthoses are typically solid plastic AFOs. This is due to the diverse functionality that they can offer. These orthoses are made with no ankle joints but allow sufficient flexibility to provide some ankle motion [6]. One of the main functions of a solid AFO is to assist in holding the foot during human gait. This happens while simultaneously providing multi-plantar motion control at the ankle joint with enough knee control. Additionally, solid AFOs help to support the ankle-foot complex within the sagittal and coronal planes. Support of knee instabilities is also provided in the sagittal plane. Even though these braces do not elevate to the height of the knee, there is some indirect support to the knee joint due to limited movement [6]. These AFOs are also applicable in respect to post-operative protection and/or support. They are capable of delivering knee stability throughout stance and control hyperextension [23]. Solid AFOs are also designated for severe ankle instability [24] and to treat Achilles tendon injuries or tendonitis as well as degenerative joint disease [25].

Leaf Spring Ankle Foot Orthoses

Leaf spring AFOs are braces made by creating a mold of a patient's leg or foot. They are a type of subject specific AFOs. These AFOs usually place the user's foot in a dorsi-flexed position during the swing phase of gait even though they are designed with a semi-flexible body that allows normal progression of the tibia throughout the stance phase of gait [6]. A particular type of leaf spring AFO is the posterior leaf spring orthosis or PLS. As the name suggests, these AFOs augment the ability of a user to perform the push-off phase in the gait cycle [26]. The main role of a PLS orthosis is to also prevent drop foot during swing in order to provide foot-ground clearance. Leaf spring AFOs are also suggested to treat lumbar spinal cord injuries [6].

Articulated Ankle Foot Orthoses

Articulated ankle foot orthoses are also referred to as dynamic AFOs. They are capable of moving about the ankle joint. Different limitations exist within the use of an articulated AFO. For instance—as a result of more mobility about the ankle joint—these braces allow forward and backward movement of the knee [6]. Additionally, articulated AFOs contain joints that offer adjustability that can be selected by the user and promote dorsiflexion and plantarflexion. These AFOs often come into play when prescribing orthotics for plantar spasticity prescriptions [27]. Finally, some CAM walkers or controlled range of motion boots also contain a revolute joint with some degree of dorsiflexion and plantarflexion. Their purpose is to accelerate recovery through muscle stimulation and still protect the affected ligaments [6].

2.2 Anatomy of the Human Foot

2.2.1 Biomechanics of the foot and Ankle

The joint of the ankle connects the foot with the lower leg. This joint actually consists of 2 separate joints which are the talocrural joint (TCJ) which represents the main ankle mortise and the subtalar joint abbreviated as (STJ). The talocrural joint articulates the distal portion of the tibia and fibula with the talus. A schematic of the talocrural joint is shown in Figure Figure 2.1. The distal point of the tibia in the medial aspect of the ankle comprises the medial malleolus, and the distal point of the fibula in the lateral aspect of the ankle forms the lateral malleolus. Throughout the gait cycle, the range of motion of the TCJ allows for dorsiflexion as the tibia advances forward when impacting the floor and plantarflexion when the heel is lifted from the ground right before toe-off. These movements are shown in Figure Figure 2.2. As for range of motion, the typical maximum flexion angles of the TCJ are 20° for dorsiflexion and 50° for plantarflexion [2], [28], [29].

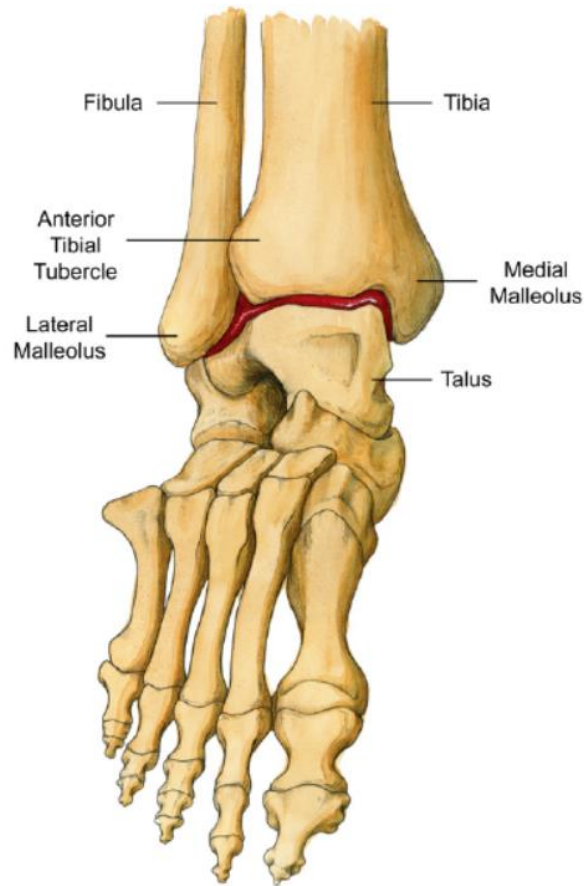


Figure 2.1 Talocrural joint (indicated by red demarcation) [30].

The STJ connects the bottom part of the talus with the heel bone which is also called the calcaneus, shown in Figure Figure 2.3. The range of motion of the STJ allows for outward heel pivoting (eversion), inward heel pivoting (inversion), foot rotation away from midline (abduction) and foot rotation towards the midline (adduction) (Figure 2.4). The range of motion for the STJ varies from 5° to 10° of eversion and 25° to 30° of inversion. Regular gait and running patterns rarely exceed these degrees of flexion. [29], [31]. In general, negligible inversion of the STJ occurs when the foot strikes on even ground, and eversion varies between 5° - 10° during 10% of the gait cycle. Subsequently, inversion at the STJ can reach up to 5° during 62% of the gait cycle [31]. The bone that connects the lower leg to the foot through the TCJ and STJ is called the talus.

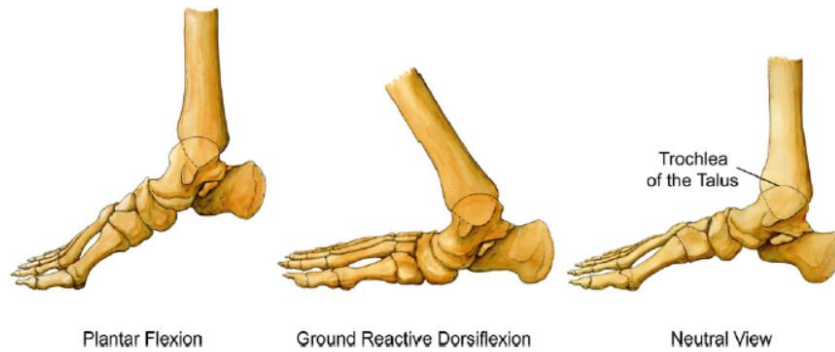


Figure 2.2 Range of motion of the TCJ [30].

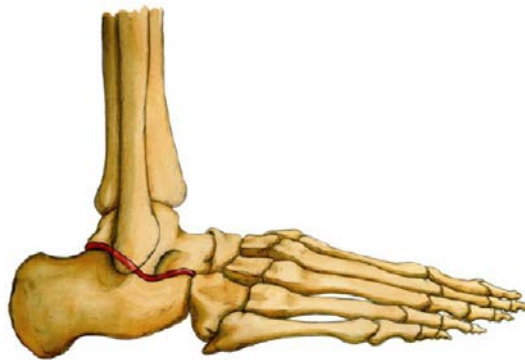


Figure 2.3 Subtalar joint (indicated by red demarcation) [30].

The soft tissue that connect bones to other bones are called ligaments. Ligaments in the ankle complex are in charge of providing passive support to the STJ and the TCJ as they come approach or go beyond the range of motion limits [2]. Bundles of collagen fibers form the ligaments. These bundles are packed in an undulating arrangement which essentially acts as springs. Each time a ligament is subjected to tension, the undulated microstructures are straightened and collagen fibers dissipate the internal forces to resist excessive stretching. Unwarranted motion of the ankle is prevented if the tension forces do not surpass the mechanical strength of the ligament. This allows the ligament to recoil back to rest. Nevertheless, if the tension force rapidly exceeds the mechanical strength of the ligament faster than corrective muscle reaction, the ligament may be subjected to microscopic tearing of the fibers or even complete rupture [12], [32].

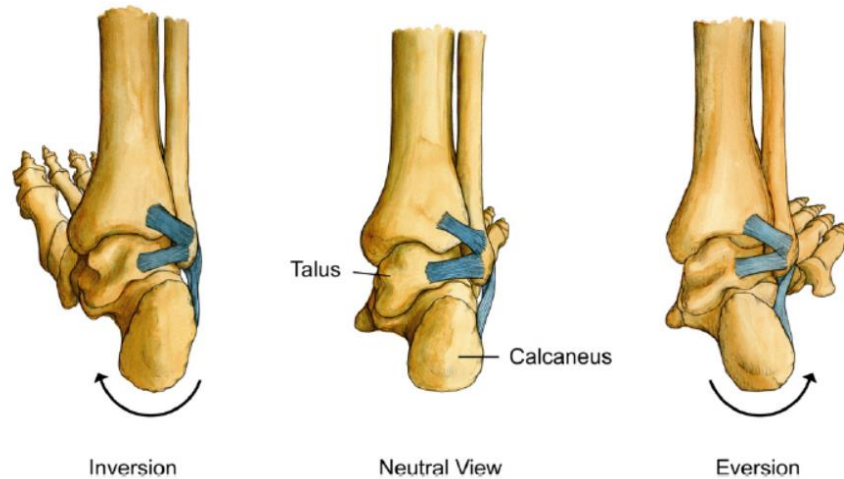


Figure 2.4 Range of motion of the STJ [30].

The principal surrounding ankle ligaments consist of the syndesmotic ligaments, the lateral collateral ligaments, and the medial collateral ligaments. The syndesmotic ligaments can be broken down into the anterior inferior tibiofibular ligament (AITFL), interosseous ligament, posterior inferior tibiofibular ligament (PITFL), and the transverse ligament. The origin of the AITFL starts at the lateral malleolus of the fibula and is distributed medially, obliquely, and proximally inserting onto the anterior lateral tibia tubercle, as shown in Figure 2.5. The interosseous ligament is encountered beneath the AITFL and it originates from the anterior inferior part of the lateral malleolus inserting onto the inferior side of the tibia. The origin of the PITFL initiates on the lateral malleolus and inserts onto the process of the posterior lateral tibia. The transverse ligament is located under the PITFL [1], [2], [12], [33], [34]. The syndesmotic ligament is in charge of supporting the fibula tightly next to the tibia, so that irregular extension of the ankle is prevented. When dorsiflexion occurs during ground impact, the posterior location of the talus rotates 5° externally inside the ankle junction. At the same time, the fibula rotates from 3° - 5° externally, and the ankle junction extends between 1-2mm [35]. The lateral collateral ligaments contain the anterior talofibular ligament (ATFL), the calcaneofibular ligament (CFL), and the posterior

talofibular ligament [1], [36]–[38], as shown in Figure 2.5. The ATFL and CFL both originate from the lateral malleolus. The ATFL inserts onto the neck of the talus and the CFL onto the calcaneus. The ATFL is responsible from resisting extreme inversion and plantar flexion of the ankle juncture, while the CFL resists unnecessary inversion of the ankle juncture and is further strained at the maximum ranges of dorsiflexion [39]. The medial collateral ligaments are composed of deep and superficial ligaments. There are two deep ligaments consisting of the anterior and posterior tibiotalar ligaments. The three superficial ligaments are the tibionavicular, tibiocalcaneal, and tibiotalar ligaments. The purpose of these ligaments is to oppose excessive eversion and external rotation of the ankle joint [1], [12], [39].

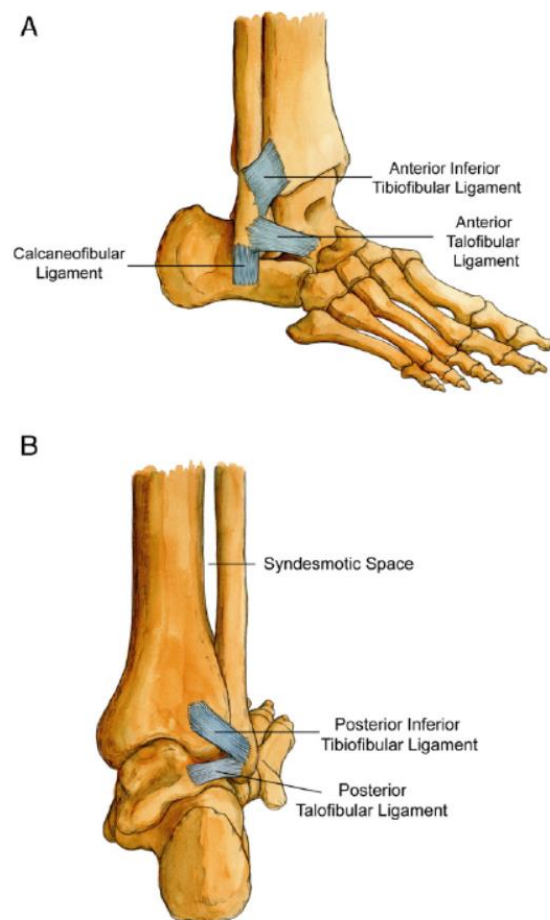


Figure 2.5 Lateral oblique view of ankle joint [30].

2.2.2 Dynamic support structures of the ankle junction

The structures that provide dynamic support to the ankle joint consist of the leg muscles, related tendons, and proprioceptive fibers encountered within the nearby arrangement of soft tissue. These proprioceptive fibers supply sensory input in terms of joint position and encourage muscle reflexes to properly move the ankle joint [12], [32], [40]. The non-elastic structures that attach bones to muscles are called tendons. Their purpose is to transfer forces generated by the attaching muscle across a joint. There are three types of contractions in which muscles generate forces: concentric, eccentric, and isometric. Concentric contractions occur when muscle fibers shorten to create a specific motion. Eccentric contractions allow for controlled lengthening of muscle fibers that decelerate motion. Isometric contractions do not involve lengthening or shortening of muscles at all. Instead, isometric contractions occur when muscles statically resist or oppose forces acting on a limb about a joint which is why isometric exercises are useful in the initial states of rehabilitation [41]. The muscles found on the outside of the leg are the peroneus longus and the peroneus brevis. The tendons of these muscles pass behind the lateral malleolus. The peroneus brevis tendon inserts onto the superior part of the fifth metatarsal while the peroneus longus passes through diagonally underneath the foot, and inserts onto the inferior surface of the medial cuneiform bone and the bottom of the first metatarsal. This is shown in Figure 2.6. The muscle situated on the front part of the shin is called the tibialis anterior and is attached to the medial-inferior feature of the medial cuneiform and the bottom of the first metatarsal bone, as shown in Figure 2.7 [42]. Concentric contractions of the peroneii musculature stimulate ankle eversion. Eccentric contractions of the tibialis anterior musculature and the nearby extensor muscles—such as the digitorum longus—help decelerate plantar flexion while concentric contractions of these same muscles stimulate dorsiflexion. A regular gait pattern is dependent on

accurate joint proprioception—or awareness of limb position and location [43]. When the swinging leg prepares to strike the ground, the lateral side of the foot has a foot clearance of only 5mm [9]. During the terminal swing phase of gait, the ideal position of the lower limb and ankle involves a slightly dorsiflexed and minimally inverted foot. Otherwise, a lateral ankle sprain is bound to occur if the outer side of the foot strikes the ground in an excessively inverted position. Several studies have cautioned that a proprioceptive peroneal muscle reaction would not be sufficiently quick in preventing an unexpected inversion sprain. Nevertheless, proprioceptive stimulation of the peroneal and tibialis anterior musculature during active gait training can help correct deficits in foot biomechanics to improve anticipation of initial ground contact [8].

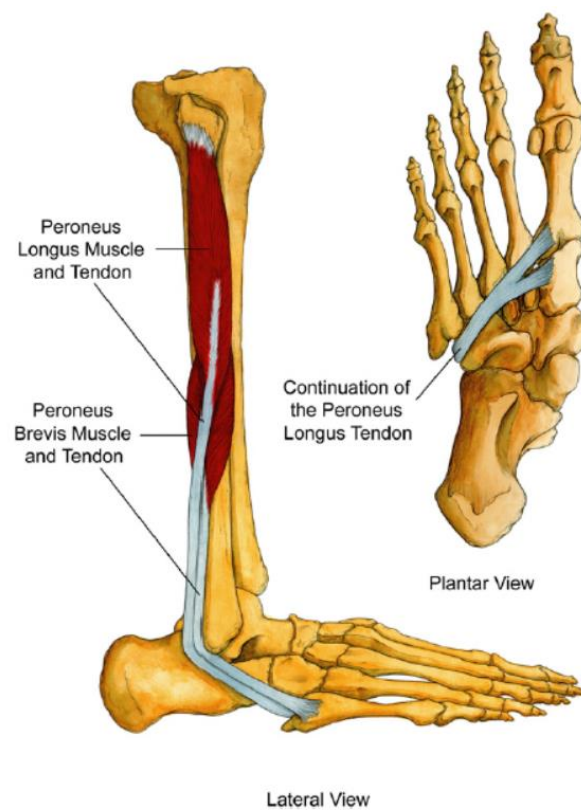


Figure 2.6 Peroneus Longus and Brevis [30].



Figure 2.7 Tibialis anterior [30].

2.2.3 Mechanisms of ankle sprains

The lateral collateral ligaments are typically injured when an individual shifts his or her center of gravity over the lateral edge of the weight bearing limb. This causes the ankle complex to quickly roll inward [44]. The weakest of the lateral collateral ligaments is the ATFL and is usually the one to be injured first[2], yet injuries to the CFL do tend to happen in more complicated sprains [45]. In sport activities, the mechanisms of injury may include landing uncomfortably on an adversary's weight bearing foot, ensnaring the outer side of the foot on the ground [46], as seen in Figure 2.8. A study that utilized cadaver ankle and foot models exposed that lateral collateral ligaments tear when the talus reaches inversion angles of around 30°-40° within the ankle junction [12]. This ligament typically fails at forces of $245 \pm 40\text{N}$ [47]. Additional injured structures that occur as a result of a lateral ankle sprain include the peroneal tendons, lateral joint capsule, and the proprioceptive nerve endings situated within these soft tissues [37], [43]. Another type of

lateral sprain that takes place in a higher area of the ankle is known as a syndesmotic sprain. These types of sprains comprise around 10% of all ankle sprains [1], [12]. Sports that involve wearing skates or rigid boots such as hokey or skiing are known to cause these types of sprains [34]. Athletes that engage in high energy contact sports such as football players can suffer from a syndesmotic sprain whenever they suddenly pivot to the inside with the outside foot fixed on the ground. Another example is that of a skier that catches the inner side of the ski while trying to avoid a gate, as shown in Figure 2.9. These two examples demonstrate the mechanisms of the injury that produce excessive external rotation on the fibula with respect to the tibia effectively disrupting the anterior inferior tibiofibular ligament or AITFL [1], [48]. The level of severity of the injury usually varies depending on the magnitude of the force on the ankle and the duration of the incident. The period of rehabilitation for syndesmotic sprains tends to be longer than lower lateral ankle injuries. A syndesmotic sprain sometimes requires a treatment that lasts almost twice as long as a grade III lateral ankle sprain [35], [49].



Figure 2.8 Mechanisms of a lateral ankle sprain and injury of ATFL [30].

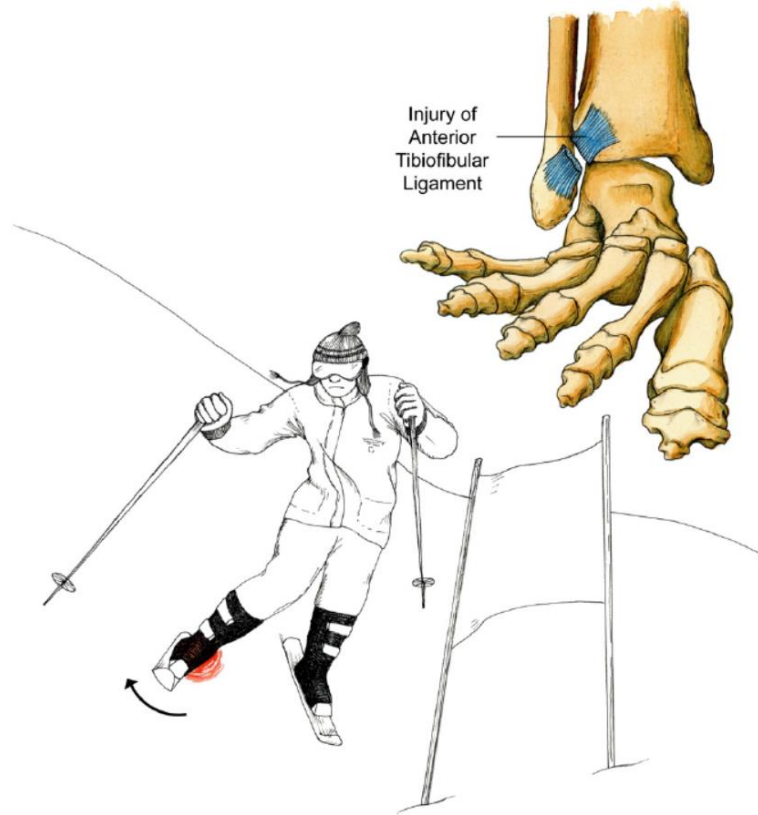


Figure 2.9 Mechanisms of a syndesmotic sprain. Injury of anterior tibiofibular ligament [30].

2.3 Human Gait Cycle

2.3.1 Definitions

The method of locomotion concerning the utilization of the two legs can be defined as gait. Before moving on, it is important to give attention to certain terms that will allow for further comprehension of human gait. A few commonly used terms include reference planes, steps/gait cycles, dorsi-flexion, and plantar-flexion. When it comes to reference planes, the typical anatomical planes used to analyze human movement are the transverse plane, frontal or coronal plane, and the sagittal plane, shown in Figure 2.10 [50].

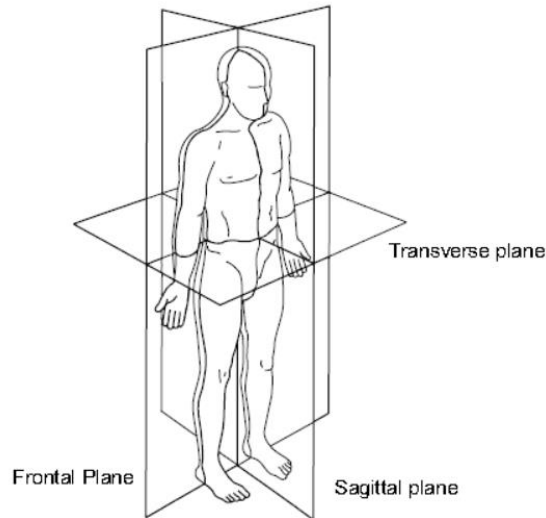


Figure 2.10 Anatomical Planes [50].

Walking is composed of recurring limb motion to propel the body onward. This is achieved while keeping a stable stance. Stride is another term that is interchangeable with gait cycle. The duration of a stride is the interval between two sequential initial floor contacts by the same limb. On the other hand an interval of initial contact with each foot is referred to as a step [51]. The difference between stride and step is shown in Figure 2.11.

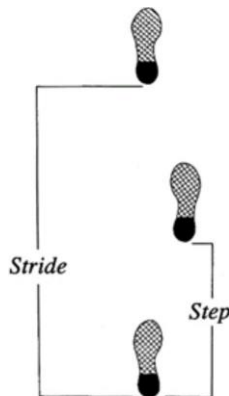


Figure 2.11 Stride vs Step [51].

In addition to steps and strides, it is also important to understand dorsi-flexion and plantar-flexion which refer to the rotation of the ankle in the sagittal plane towards or away of the body respectively, as displayed in Figure 2.12.

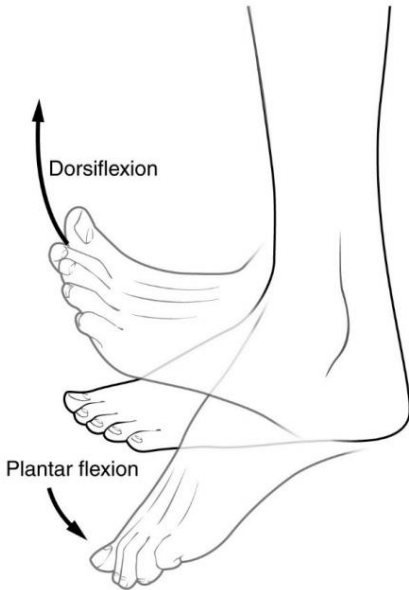


Figure 2.12 Plantar-flexion and dorsi-flexion [52].

2.3.2 Gait Phases

The gait cycle can be broken down into eight phases, this allows for the limb to complete three basic tasks which are weight acceptance, single limb support, and limb advancement as shown in Figure 2.13 [51].

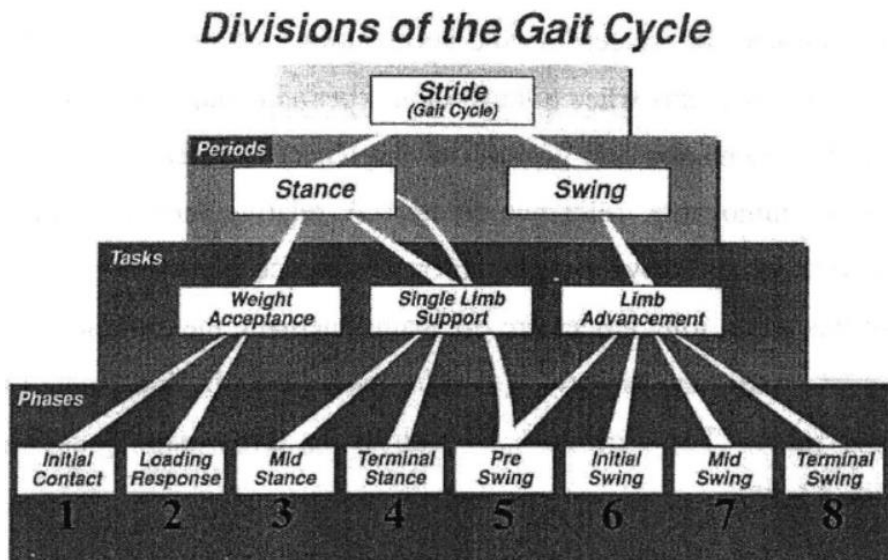


Figure 2.13 Divisions of the gait cycle [51].

Weight Acceptance

The most demanding task in the walk cycle is weight acceptance, as shown in Figure 2.14 since it demands an abrupt transfer of body weight onto the limb that recently finished swinging forward. It requires shock absorption of the free-falling body, a stable stance limb, and preservation of onward momentum. The two walk phases that comprise this task are the initial contact and loading response.

Phase 1 (Initial Contact)

It occurs the instant the heel touches the floor. It represents approximately 2% of the gait cycle. During initial contact (IC). When this happens, the hip is flexed at around 30°. Additionally, the ankle is dorsiflexed to a neutral position while the knee is completely extended.

Phase 2 (Loading Response)

Consisting of about 10% of the gait cycle and together with the initial contact of the foot this phase continues until the other foot begins to raise for pre-swing. This phase is also distinguished by the heel-to-floor shock absorption and by the load acceptance. The body weight is transferred onto the reference limb and the heel acts as a rocker allowing the knee to be flexed for shock absorption.

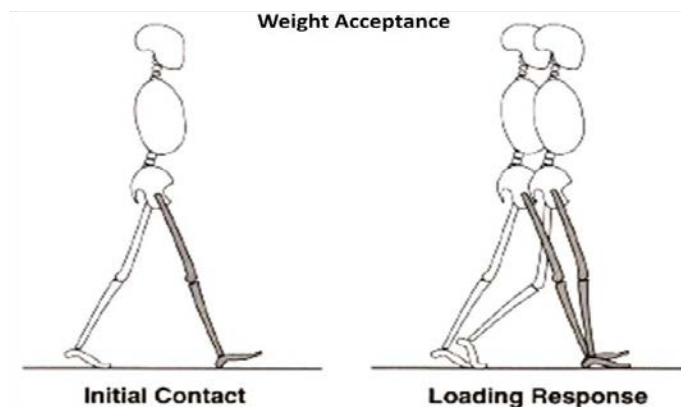


Figure 2.14 Weight Acceptance [51].

Single Limb Support

This task starts when the trailing foot is being lifted for swing and continues until the same foot contacts the floor. Consequently, the reference limb is responsible for supporting the body weight in the coronal and sagittal planes as can be observed in Figure 2.15. There are three walk phases included in this stage: Mid Stance, Terminal Stance, and Pre-Swing (of reference limb).

Phase 3 (Mid Stance)

During the Mid Stance phase, the reference limb advances the entire body forward while the ankle is in dorsiflexion permitting the flexed knee to extend along with the hip. In the meantime, the trailing limb advances in its mid-swing phase in the coronal plane. The mid stance phase takes up an interval of 10% -30% of the gait cycle.

Phase 4 (Terminal Stance)

This phase occurs when the heel of the reference limb starts to rise. The knee continues to extend and then begins to flex to some extent until the other limb finishes its swinging phase and strikes the ground. Moreover, this phase falls between the interval of 30%-50% of the gait cycle.

Phase 5 (Pre Swing)

Representing 50%-60% of the gait cycle, this is the final phase of the stance and the beginning of the swing for the reference limb. This phase starts with the initial contact of the opposite limb's heel and the toes of the reference limb are immediately raised. Here the body weight is unloaded from the reference limb and transferred to the opposite limb which will now begin its loading response. The reference leg will now begin its swing period with increased ankle plantarflexion, knee flexion, and no hip extension.

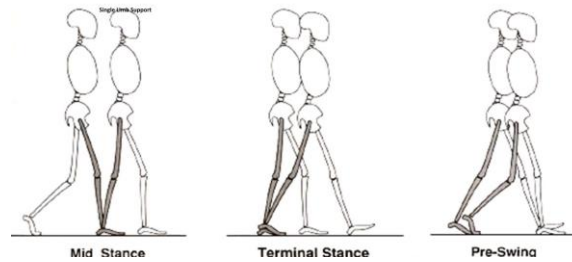


Figure 2.15 Mid stance, terminal stance, and pre-swing phase [51].

Limb Advancement

Phase 6 (Initial Swing)

As the reference foot is lifted from the ground, the initial swing ends when this same limb is next to the opposite foot which should be in the stance phase. The swinging reference leg displays increased knee flexion around 60° avoiding dragging of the foot because of the loss of hip extension. This allows the limb to propel forward like a pendulum. All of this occurs in the interval of 60%-70% of the stride.

Phase 7 (Mid Swing)

This phase starts when the reference limb is swinging and positioned next to the opposite stance leg. It proceeds until the swinging reference leg is further ahead of the opposite leg and the flexion angles of the hip and knees are equal. This occurs at 70%-85% of the stride. It ends when the flexion angle of the knee decreases to 30° .

Phase 8 (Terminal Swing)

The knee of the reference leg is fully extended and the swing is completed. In this last phase, everything starts when the hip keeps its flexion angle and the ankle stays dorsiflexed in a neutral position. The end of the phase happens when the reference limb makes contact once again with the ground re-starting the cycle and placing the opposite limb in terminal stance. The terminal swing phase comprises an interval of 87%-100% of the gait cycle. (All cycles [51]).

2.3.3 Analysis of Gait

A typical gait is a rhythmic process, and it consists of alternating propulsive and restraining motions of the lower extremities [53]. Gait can be used to describe different types of gait patterns such as walking, waddling, running, and gaits with physical limitations. This thesis however, will put emphasis on normal walking.

2.3.4 Kinematics of Gait

In order to differentiate between normal gait and pathological walking it is essential to obtain measurements of joint angular rotations and translations of the limbs and the entire body [54]. Analyzing the kinematics of gait provides useful information of objects in motion disregarding the causes of such motions [55]. Special attention is given to joint motion, linear and angular displacements, velocities, and accelerations of the limbs. There are multiple strategies that can be taken to obtain such measurements. Some strategies consist of utilizing goniometers, accelerometers, and resistive grid walkways. These are often referred to as “direct measurements” [51], [56]. However, while these techniques are useful for certain studies; they can be difficult to implement and lead to scarce information. Another technique used for kinematic data acquisition is the “imaging method” which consists of placing reflective markers on the limbs and recording the subjects with motion capture video. This method produces three-dimensional kinematic data. Multiple cameras placed around the subject track a 2-D position of each reflective marker [57]. The combined information of each camera generates a position estimation of each reflective marker in 3D space, giving scientists the ability to calculate joint angles, velocities, and accelerations.

2.3.5 Kinetics of Gait

The factors that result in movement while mainly looking at the forces involved are points of interest in the study of kinetics [55]. The joint moments and powers of limbs are typically addressed in kinetic and dynamic analyses. Muscle excitation, joint and structural limitations as well as ligamentous constraints produce internal moments whereas the ground reaction forces (GRF) generate external moments on the joints. In general, the principal external forces involved in human locomotion are gravity and the GRF between the floor and the ground [58]. Horizontal and vertical component forces can be identified from the ground reaction of the bottom of the foot impacting the surface. Additionally, the horizontal component of the GRF can be described by a mediolateral and anteroposterior components that correspond to friction [59]. In order to obtain a kinetic or dynamic analysis, the location of the joints and the external forces acting on the body are required. Kinematic analysis gives the location of the joints and external forces are typically obtained with force plate measurements [60]. Force plates are utilized to acquire gaugeable information of the vertical direction reaction forces. These plates also provide information of the center of pressure propagation, shear forces along the surface of the plane, and moments about any axis [61].

2.3.6 Electromyography

Throughout muscle function, electric signals are produced and with the help of electrodes it is possible to record such signals. The process of recording the electrical activity of a contracting muscle is called Electromyography (EMG). Presently, an EMG system can show electrical impulses as wavelike tracings on a graph using a computer, but it traditionally involved the use of cathode-ray oscilloscopes [62]. There are two major types of electrodes used in EMG, surface electrodes and intramuscular wire electrode. Preference is widely given to surface electrodes due

to the simplicity of their application and the skin is not pierced as is the case with intramuscular wire electrodes. Normally, EMG data is recorded with either active or passive surface electrodes. An amplifier is built into active electrodes and are less exposed to noise or interference caused by wire movement. It's important to point out that surface electrodes cannot be used to detect deep muscle activity. Furthermore, surface electrodes tend to pick up signals from adjacent muscles of no interest. This is known as cross-talk and it happens when small muscles next to larger muscles undergo overlaying excitation patterns. To avoid cross-talk, fine wire electrodes are used since they have the advantage of precise deep muscle placement. Essentially, everything depends on what muscles are being studied and whether non-invasive alternatives are required which would demand the use of surface electrodes [63].

2.4 Critical Review of Topics Pertaining Gait with Foot Orthoses

Throughout time, different models describing the interaction between the human foot and AFOs have been created with distinctive purposes such as analyzing kinematic and kinetic data, obtaining electromyography and energy expenditure information, treatment abnormalities, and multibody dynamics simulations (limb/orthoses interface loads). This literature review provides a summary of some of the different musculoskeletal models done throughout the years.

2.4.1 AFO Ground Reaction Forces (Kinetics and Kinematics)

Ground reaction forces and body movement are amongst the primary types of studies conducted in biomechanics. The use of force plates and motion capture systems allows scientists to analyze the principles of kinetics and kinematics. Naturally, the effects of an AFO became a topic of study for many authors, as was the case of Zhang, et al, in their study titled “Ground reaction force and 3D biomechanical characteristics of walking in short-leg walkers” [64]. Their recognized that short-leg walking boots present multiple advantages over conventional casts.

Nevertheless, they also acknowledged that effects that short leg boots have on ground reaction forces and 3D biomechanics are not fully understood. For this reason, the team examined 3D joint dynamics and lower extremity kinematics during gait with two different designs of short-leg walking boots. Eleven subjects with no injuries performed five trials in each of the three conditions which were: wearing a pair of lab shoes and two different boots, GaitWalker and Equalizer. The male to female subject ratio was 6:5. By placing a pair of photocells at the height of the shoulders and using three walking trails at a selected speed, the average walking speed of each subject was obtained. The speed of the subject gait was monitored to make sure it was within ten percent of the mean walking speed. The conditions of the boot were structured in such a way that one of the walkers would always be tested first and the shoe condition would be tested at the end. This was to get the preferred walking speed. A force plate and a motion analysis system (Vicon, six cameras) were utilized to obtain space kinematic and ground reaction forces data during testing sessions. By using a fourth-order Butterworth low-pass filter, data was smoothed at 6 and 20 Hz, for the kinematic and ground reaction forces respectively. Visual3D suite was used to compute the variables for the space kinematics as well as the kinetic variables. Ground reaction forces together with joint moments were normalized to each of the participants' body mass. This resulted in the following units: N/kg and N m/kg, respectively. The reflective markers for the medial and lateral malleolar were placed on the medial and lateral side arms of the walkers. Two virtual markers were used to define the location of the ankle after measurements the widths of the ankle with and without wearing the walker with a caliper. In order to expose the skin for the attachment of reflective markers on the foot, the linen wrap inside the walkers was cut at the heel and lateral aspects of the mid and anterior walkers. No alterations were made to the straps of the walker and this help to maintain its integrity. The reflective marker placement is shown in Figure 2.16.



Figure 2.16 Reflective markers placement on lower extremity and pelvis [64].

An ANOVA was utilized to scrutinize the selected ground reaction forces, joint kinetic variables, and kinematics with a p value of < 0.05 . The results showed that both of the short-leg walking boots were effective in minimizing ankle eversion and hip adduction. It is important to note that neither walker increased the bimodal vertical ground reaction peaks that are detected in normal walking. However, they did impose a small initial peak of < 1 BW earlier in the stance phase. Both walkers seemed to increase the recruitment of the knee extensors but decreased the demand of the knee and hip abductors according to the joint kinetic results. The ground reaction forces and joint moments are displayed in Figure 2.17.

As a whole, the research served as supplemental information on the subject of biomechanics of short-leg walking boots by implementing pre-existing methodologies for calculating ground reaction forces. Monitoring the walking speed is a good approach as it will allow for a better representation of the gait cycle avoiding different step and stride distances which could lead unwanted variability in the data.

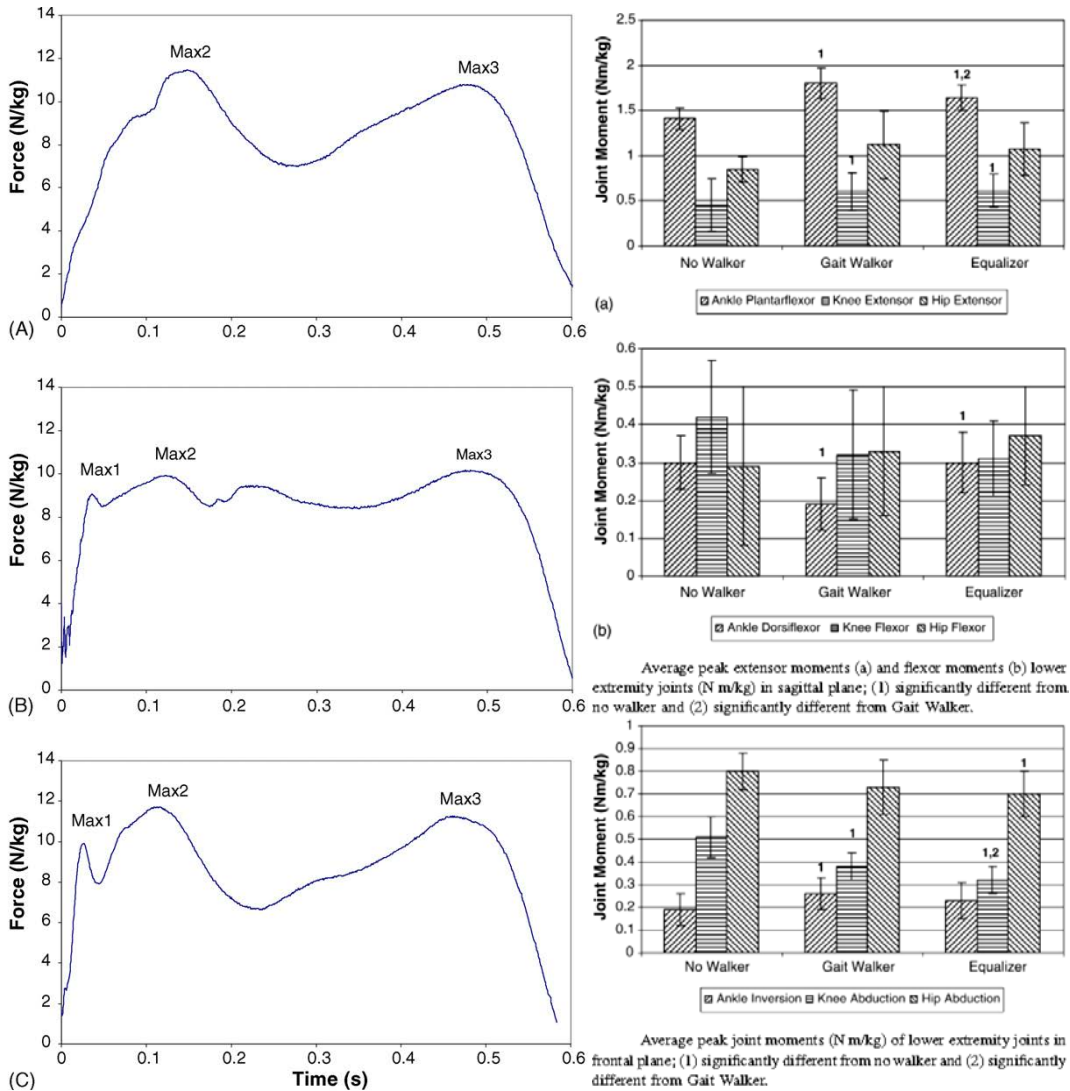


Figure 2.17 Ground reaction forces and joint moments [64].

The obtained results were in comparison are consistent with the magnitude of the reaction forces during a gait cycle as well as with the joint moments. While the purpose of the study was met, new questions can be formulated to further study the effects of ground reaction forces on the AFO and how these affect the comfort of the patient. For instance, what causes the Max 1 GRF peaks found on both walkers? And what types of complications—if any—can these forces create for the injured patient during the rehabilitation process?

Two years later, the authors decided to address these questions in a supplementary study titled “Effects of modified short-leg walkers on ground reaction force characteristics” [65]. In this study the authors pointed out that even though short leg walkers are constantly used to treat injuries in the lower extremities such as ankle and foot fractures as well as level 3 ankle sprains, there is still a lack of knowledge regarding the effect that short leg walkers have on the gait patterns. The main intention of their new study was to analyze how modifications of heel height in different walkers and shoe side could disturb the GRF in walking. One of the expectations was to see that minimizing artificial leg length discrepancy by applying a short-leg walker with an insert or shoe side would cause GRFs to match closely with GRFs found when wearing normal shoes. The other expectation was that a greater heel-to-forefoot height ratio would also cause GRFs to appear more similar to gait patterns found with normal shoes. This was of course, an extension of previous study done by Zhang et al., 2006 [64]. Force plates collected GRF data on 10 healthy subjects. There were six conditions on which five trials were executed: lab shoes, gait walker, gait walker with heel insert on shoe side, modified gait walker with insert on walker side, equalizer walker, and equalizer walker with heel insert on shoes side. The equalizer walker is shown in Figure 2.18. The right leg was used for all of the walker conditions with lab shoes worn on the left leg. The padding and small slits were cut out from the walkers in order to access the foot and allow the placement of a plantar pressure sensor arm. The medial arm and Velcro straps of the walkers were left intact. The forefoot heights and heel for the walkers and shoes were measured with the use of an anthropometer. The measurements for the height were taken at the approximate location of the third metatarsal head on the insole for the forefoot. For the heel height, the middle heel region height was used. These dimensions were used to create inserts that modified the heel-to-forefoot height ration. Samples of the insole material were obtained from the heel region for the equalizer

and the gait walker. Deformation testing was performed and the average deformation results was taken to manufacture inserts for the gait walker with the purpose of achieving a desired heel-to-forefoot height ratio. The desired heel-to-forefoot ratio was proposed from the previous study Zhang, et al., 2006 [64]. The heel-to-forefoot height ratio for equalizer was 1.49 and was proposed to be linked to a smoother transition from heel-strike to toe-off. As a result, the heel inserts were created for the gait walker to replicate the targeted ratio of 1.50 as was calculated for the equalizer's heel-to-forefoot height ratio. Three pieces of coring foam were cut, glued, and ground to match the contour of the heel in order to create the heel insert for the gait walker. The height of the heel inserts was tapered down to 60 percent of the foot length. Heel inserts were added to the walkers' sole with double sided tape and further secured to the walker by applying Velcro straps on the walkers. Shoe inserts were made to eliminate the artificial limb length difference created with the application of the short-leg walker between the shoe and walker sides during walker testing conditions. A foam piece ground down and then glued underneath an off-shelf shoe insert was used to manufacture each individual insert.



2.18 Two short-leg walkers used in the study: gait walker (A) and equalizer (B) [65].

A repeated 2 by 6 ANOVA study was used on the selected GRFs with ($p < 0.05$). The length of the limb was measured with subjects placed in a supine position. These dimension were obtained measuring the distance from the medial malleolus to the superior iliac spine on both limbs. The ground reaction data was collected with 2 force-plates. Two photocells were utilized together with a timer to supervise gait velocity. Peak vertical and anteroposterior GRFs were generated when the walker was applied. This occurred right before the typical peaks associated with the loading phase. Also, compared to the shoe on the walker side, an elevated minimum vertical GRF was introduced by wearing a walker in all conditions excluding the equalizer walker. Furthermore, contrary to what was hypothesized, there was evidence that vertical GRFs did not diminish with inserts applied to both the gait walker and the shoe side, and modifying the gait walker. Finally, peak propulsive anteroposterior GRFs seemed to decrease on the walker side and also induce asymmetrical loading. The results in regards to GRFs are shown in Table 2.1. The mean minimum vertical GRFs, mean peak breaking forces, and mean peak propulsion forces are shown in Figure 2.19.

Table 2.1 Mean Peak Vertical GRFs and Time to Peaks Mean (SD) [65]

Mean peak vertical GRFs and time to peaks: mean (SD)					
Side	Condition	F2 ^b (BW)	T2 (s)	F3 (BW)	T3 ^b (s)
L	Shoe	1.146 (0.09)*	0.183 (0.03)	1.151 (0.08)	0.555 (0.03)
	GW	1.120 (0.09)	0.343 (0.14)	1.153 (0.09)	0.562 (0.06)
	GWII	1.127 (0.07)	0.272 (0.12)	1.129 (0.08)	0.761 (0.28)
	GWM	1.131 (0.10)	0.339 (0.15)	1.145 (0.10)	0.577 (0.05)
	EW	1.125 (0.08)	0.275 (0.10)	1.149 (0.08)	0.597 (0.05)* ^a
	EWHI	1.135 (0.07)	0.301 (0.14)	1.140 (0.08)	0.583 (0.04)
R	Shoe	1.101 (0.08)	0.239 (0.12)	1.135 (0.08)	0.367 (0.03)
	GW	1.154 (0.08)	0.301 (0.12)	1.005 (0.36)	0.517 (0.19)
	GWIII	1.153 (0.07)	0.261 (0.08)	1.130 (0.08)	0.555 (0.05)
	GWM	1.122 (0.08)	0.292 (0.09)	1.101 (0.08)	0.579 (0.06)
	EW	1.107 (0.07)	0.249 (0.07)	1.113 (0.05)	0.568 (0.04)
	EWHI	1.123 (0.05)	0.240 (0.07)	1.136 (0.06)	0.360 (0.04)

Note: F2 – peak vertical GRF associated with loading response.

T2 – time from contact to F2.

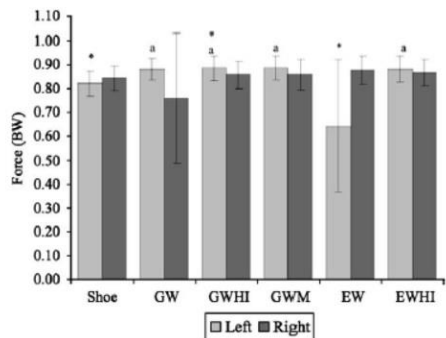
F3 – peak vertical GRF associated with push-off

T3 – time from contact to F3.

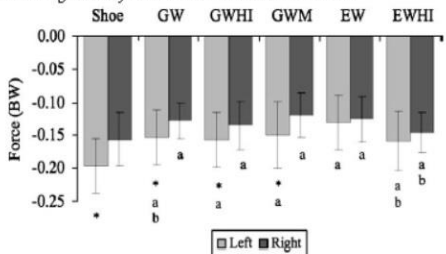
* Significantly different from the right side of the same condition.

^a Significantly different from shoe of the same side.

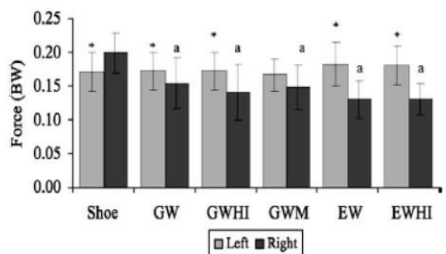
^b Significant side by condition interaction.



Mean minimum vertical GRF (Fmin) during midstance: * - significantly different between the left and right side of the same condition and a - significantly different from shoe of the same side.



Mean peak breaking GRF (Fb): * - significantly different from the right side of the same condition, a - significantly different from shoe of the same side and b - significantly different from EW of the same side.



Mean peak propulsion GRF (Fp): * - significantly different between left and right side of the same condition and a - significantly different from shoe of the same side.

Figure 2.19 Mean minimum GRFs, mean peak breaking force, & mean peak propulsion force [65].

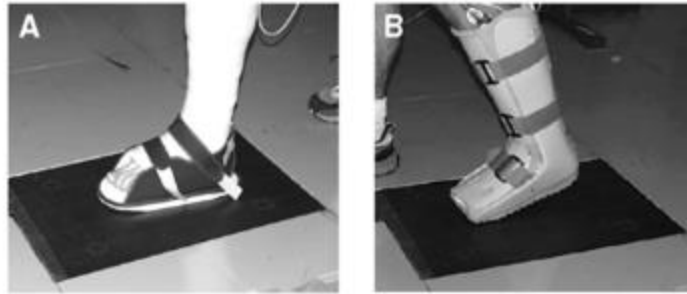
In general, the authors attempted to address the peak ground reaction forces that were present in their last study. Their methodology to minimize artificial leg length discrepancy and atypical GRF by introducing sole inserts seems logical since there is still debate regarding the similarities between true limb length discrepancy and artificial limb length discrepancy as well as which limb is receiving more of the load. The results of this study were unexpected not only for the reader but also the authors given that an initial F1 peak GRF was also present on the shoe side in some

subjects. Additionally, some significant difference was present in the case where there was no limb length discrepancy. The author proposed that this could have been due to subjects getting used to different conditions' gait characteristics. The authors also stated they tried to control for this by allowing participants time to become accustomed to each condition. Just as the authors pointed out, the hypothesis was not verified; the modifications that were made did not eliminate atypical initial peak forces. Modifications used to decrease limb length discrepancy created by the application of a walker did not return GRFs to those seen in normal shoes.

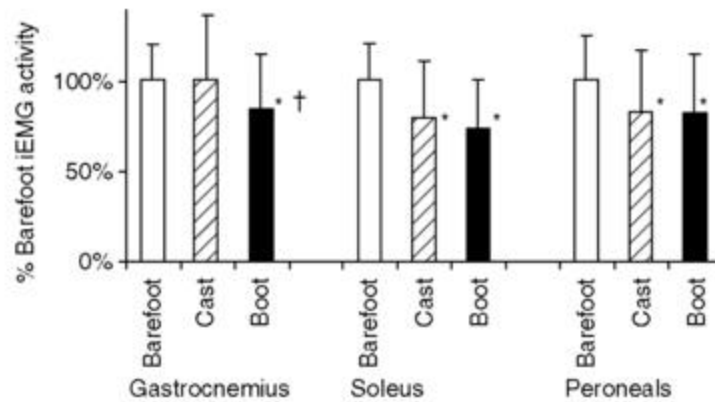
2.4.2 Work/Energy expenditure and use of electromyography with AFOs

Other types of studies performed in biomechanics research deal with work and energy expenditure and the typical approach consists of operating electromyography equipment in order to obtain muscle activation data. An example is the research that Kadel, et al, performed in their study called "The Efficacy of Two Methods of Ankle Immobilization in Reducing Gastrocnemius, Soleus, and Peroneal Muscle Activity During Stance Phase of Gait" [66]. The rationale behind this study was to compare if the reduction of muscular activity between a fiberglass cast versus a prefabricated off the shelf boot. EMG data was captured from the gastrocnemius, soleus, and peroneals of 12 normal adults while walking barefoot in three different conditions: walking barefoot, wearing a fiberglass cast with a cast shoe, and wearing an Aircast FoamWalker boot. The motivation for this study was that no comparisons had been made between custom applied casts and commercially available boots. The authors' hypothesis was that an off the shelf boot was as effective as a custom applied cast in reducing plantarflexor contractile activity while walking. Eight men and four women without any known pathology were recruited for the study. The muscles chosen for the EMG surface electrodes were the left medial gastrocnemius, lateral soleus, and peroneal muscles. The lower leg was wrapped to secure the electrodes and leads. A goniometer

was used to verify that 90° dorsiflexion was used during the cast application. Subjects practiced walking at a self-selected speed. Electromyography activity was obtained and sampled at 2100 Hz and a low-pass filter was applied at 350 Hz. A total of 10 walking trials were taken for the EMG and force plate data acquisition under each of the three conditions. Force data was only use for stance phase reference. EMG data was then rectified and normalized to a percent of each subject's barefoot mean. A post hoc linear contrast analysis was used to compare differences between boot and barefoot, between cast and barefoot, and between boot and cast trials. Between the barefoot and boot conditions, a significant decrease in muscle activity was observed for the three muscles in question: gastrocnemius ($p=0.04$), soleus ($p < 0.0001$), and peroneals ($p=0.02$). The comparison between barefoot and cast had a non-significant reduction of the gastrocnemius activity ($p=0.9$), but it did however show a significant decrease in the soleus and peroneal activity ($p=0.006$) and ($p=0.01$) respectively. The comparison between the boot and the cast showed a decrease in the activity of the gastrocnemius in the boot compared with the cast ($p < 0.0001$), but no significant difference happened between the boot and cast for the soleus ($p=0.5$) or peroneals ($p=0.7$). The results of this study demonstrated that the effectiveness muscle activity reduction of a prefabricated walking boot is comparable to that of a custom-made fiberglass cast (Figure 2.20). Additionally, the experiments showed that the boot is superior to the cast in decreasing muscle activity of the gastrocnemius. An overall muscle activity reduction of 20% occurred when using the boot.



Subjects walked across a force plate in a cast with a cast shoe (A) or a walking boot (B).



Mean (+SD) iEMG levels for the barefoot, cast, and boot conditions, expressed as a percent of barefoot activity. *indicates significant difference from barefoot value at $p < .05$; †indicates significant difference from cast value at $p < .001$.

Figure 2.20 EMG activity of 3 conditions as percent of barefoot activity [66].

In summary, the authors suggested that prefabricated boots can be used as an alternative to custom applied casts when the clinical objective is to decrease muscle activity of the calf. Yet some weaknesses of the study were that there was no control or measure for walking speed, and that the rocker bottom of the cast and boot were different. The failure to significantly reduce the activity of the gastrocnemius in the cast could have been due to a less effective rocker bottom in the cast compared to the walking boot. It is possible that a reduction in the walking speed while wearing the cast and the boot compared to barefoot could have contributed to different EMG activity.

Fröberg, Åsa, et al. decided to use a more invasive type of EMG analysis to study the forces in the Achilles tendon. Their study was titled “*Force in the Achilles tendon during Walking with Ankle Foot Orthosis*” [67]. The aim of this study was to determine whether the Achilles tendon load would decrease with increased restriction of dorsiflexion and if such restrictions would also decrease triceps surae activity. Tendon force transducers were used for the determination of tendon loading differences between different AFO settings. An optic fiber technique was applied in this study to measure the load on the Achilles tendon during walking in an AFO set in 3 different positions used in standard rehabilitation protocols. The research also revised previous studies which stated that postoperatively, the ankle is traditionally placed in plantar flexion as it is believed that this will assist in adapting the ends of the ruptured tendon after suture. A total of 8 healthy subjects (5 females and 3 males) participated in the study. Muscle activity for the medial gastrocnemius, soleus, and tibialis anterior was recorded. The electrode placement for the soleus was located halfway between the gastrocnemius and the point of insertion of the soleus in the Achilles tendon. A cannula with a thickness of 1.1mm was inserted in the Achilles tendon, as shown in Figure 2.21. A polymethyl methacrylate optic fiber with 0.5mm thickness and 1 m in length was threaded through the cannula. Afterwards the cannula was removed leaving the optic fiber in the tendon. The fiber ends were cleaned and attached to a light emitting diode and a pin-type photodiode receiver. Tendon deformation during measurements modulated the light intensity going through the fiber. The light signal picked up by the receiver was transformed into an analog signal and recorded by computer. The optic fiber signal was calibrated in comparison to a strain gauge force transducer during plantar flexion. The calculated external force represented Achilles tendon force (ATF). The subjects walked along a 10m force plate at their own speed. The subjects were then instructed to wear an AFO. At first, the AFO was set to allow free plantar flexion with

restricted dorsiflexion to 10° of plantar flexion (10° PF). Afterwards, the orthosis set to allow plantar flexion but restricted dorsiflexion to 10° of dorsiflexion (10° DF). Then the orthosis was fixed with no range of motion at 20° of plantar flexion (20° PF). A setting of 20° pf was used in the study instead of the 30° used in the hospital protocol because 30° of ankle plantar flexion increased the risk of interference between the optic fiber and the orthosis. Information from the optic fiber, the EMG, and the force plate was transferred through an A-D converter at a sampling rate of 1013.1Hz to a Victor Sirius microcomputer for analysis.



Figure 2.21 Insertion of cannula in tendon [67].

Representative mean Achilles tendon ground-reaction force, and EMG curves for one subject are shown in the Figure 2.22. The Achilles tendon mean peak forces and mean force rate are shown in Figure 2.23, at ± 95 confidence interval as a factor of body weight and N/s, respectively. In these graphs pf stands for plantar-flexion; df, dorsiflexion; and bf, barefoot. Figure 2.24 displays the mean EMG activity of the soleus, gastrocnemius, and tibialis anterior muscles at a ± 95 confidence interval expressed as a percentage of mean activity during barefoot walking. In other words, the mean activity found during walking is set to 100%.

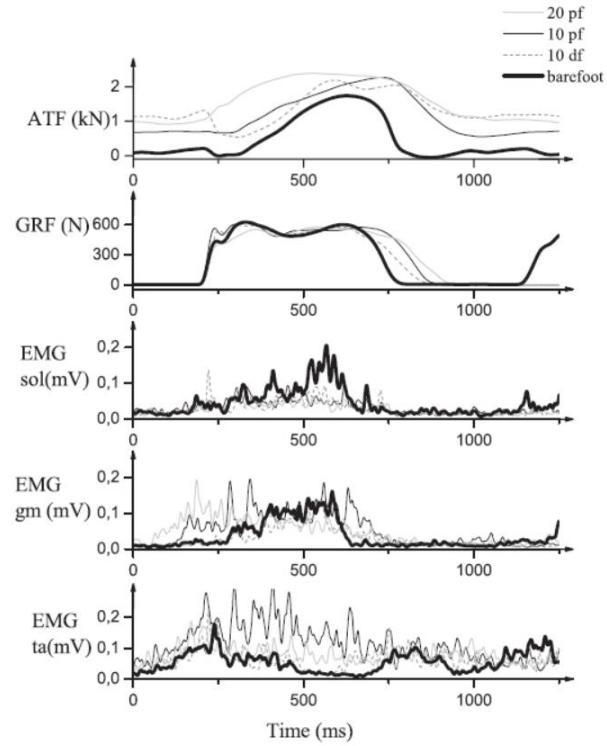


Figure 2.22 Achilles tendon mean force curve and EMG activity [67].

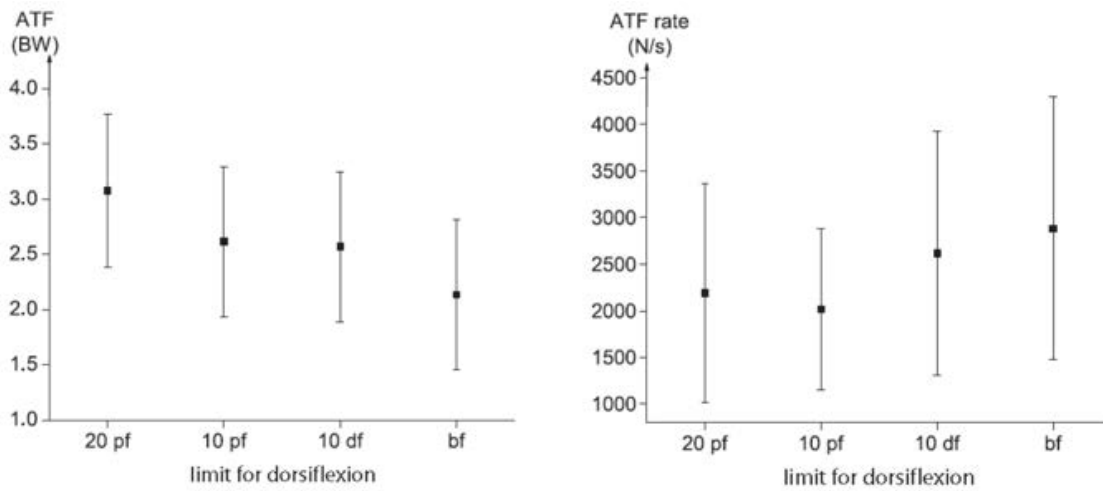


Figure 2.23 Achilles tendon mean force and mean rate [67].

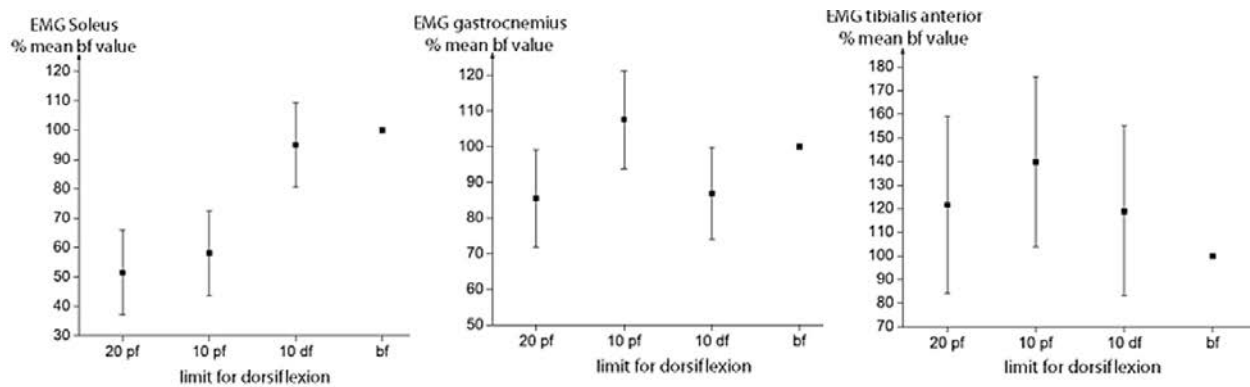


Figure 2.24 Mean EMG activity of the soleus, gastrocnemius, and tibialis anterior muscles at a ± 95 confidence [67].

Studying Figure 2.23, it can be seen that the ATF mean force gradually decreased as restriction in dorsiflexion lessened from a factor of 3.1 times body weight at an AFO setting 20° plantarflexion (PF) to 2.1 times body weight during barefoot walking. Soleus activity gradually increased as dorsiflexion limitation decreased (Figure 2.24). EMG activity of the soleus was 52% of barefoot walking activity at 20° PF, 58% at 10° PF, and 95% at 10° DF. Activity in the gastrocnemius muscle varied from 85% at setting 20° DF to 108% at setting 10° PF and 87% at AFO setting 10° DF (Figure 2.24). Muscle activity for the tibialis anterior at 10° PF (Figure 2.24) was 140%, which was significantly higher than during barefoot walking. Interestingly enough, walking rate was not controlled given that subjects were instructed to walk as relaxed as possible at their own preferred speed. However, the authors stated that no statistical difference was found in walking speed between the different walking conditions, so it is not likely that this had a major influence on the results. The ATF peak was shown to be significantly higher at AFO setting 20° PF as compared with barefoot walking. According to treatment protocols the chosen setting is used when the plaster cast is removed 2 weeks postoperatively. During this rehabilitation stage, patients are told to use crutches to relieve load from the Achilles tendon during gait, in this study however, no crutches were used and full weight-bearing was allowed. The important thing to take from this

study is that if a patient were to accidentally or deliberately support on his or her foot while the AFO was locked at 20° PF, the loading on the tendon may exceed loading usually encountered during barefoot walking.

2.4.3 Conclusion and Research Proposal

This literature review presented a detailed introduction to foot orthoses, the anatomy of the human foot, the mechanisms of ankle sprains, and the characteristics of human gait. Subsequently, various studies pertaining to biomechanics of ankle foot orthoses were discussed. While these studies analyzed the effects of rigid and functional articulated AFOs on muscle activity, it is evident that the integrity of the affected ligaments during conservative and functional treatments of ankle sprains is a subject that is not completely agreed upon. Therefore, examining the appropriateness of functional treatment with regards to inversion ankle sprains can help shed light on its role in stimulating sprain-preventive muscle reflexes that improve ankle control and function.

CHAPTER THREE

METHODS

3.1 Subjects

Written informed consent was obtained from 10 healthy subjects (male to female ratio 5:5) who volunteered for the study. The weight of the subjects ranged from 48.53 TO 88.45 kg (mean 68.31). Subjects did not have any mobility limitations that would affect their ability to walk. The experimental protocol was approved by the Wichita State University Human Subjects Institutional Review Board.

3.2 Experimental Protocols

Kinematic, kinetic, and electromyographic (EMG) data were collected from healthy college-aged subjects as they walked on six force plates arranged in a staggered configuration in the center of the Biomechanics Laboratory (Figure 3.1). Three conditions of gait were used for the experiment: i) regular walking (No Boot), ii) rigid CAM Walker boot (0° Plantar-flexion/Dorsi-flexion), and iii) CAM Walker with range of motion of 20° plantar-flexion and dorsi-flexion. EMG data were collected using surface electrodes from three superficial muscles: right tibialis anterior, right extensor digitorum longus, and right peroneus longus. The rationale behind choosing these muscles is due to the fact that the tibialis anterior and extensor digitorum longus are in charge of dorsiflexion while the peroneus longus control eversion and plantarflexion. These movements are necessary for proper motor control, stability, and ground clearance to avoid recurring inversion sprains. During the experiment subjects dressed in tight clothing to help identify bony landmarks. For the static trial, subjects were instructed to stand stationary in anatomical position. For the walking trials, subjects were instructed to walk under the 3 conditions as naturally as possible while trying to land one foot on at least one of the 6 force plates in the lab. Subjects performed 5

trials for each of the conditions mentioned above for a total of 15 gait trials per subject (or 150 trials total). The order of the conditions was meant to be randomly assigned, but consideration was given to subjects' time availability and as a result the order was structured to move from regular gait to wearing the boot and subsequently adjust the boot's range of motion:

1. No boot,
2. 0° plantar-flexion/dorsi-flexion,
3. 20° plantar-flexion/dorsi-flexion.

The entire experiment took approximately one and a half hours per subject. One trial from each walking condition was used to generate a computed muscle control simulation.



Figure 3.1 Biomechanics Laboratory

3.3 Equipment

Kinematic data were collected using an 11-camera video based motion analysis system and Cortexv5.3 software (Motion Analysis Corp., Santa Rosa, CA). A marker set (27 retro-reflective markers) was used to define the foot, shank, thigh, pelvis, torso, and head segments for each subject for the standing static pose and walking motion used (Figure 3.2). Reflective markers for the heel, and lateral/medial malleolus were placed on the surface of the boot for the rigid AFO and

articulated AFO conditions. As a result, 3 virtual markers were created in Cortex to estimate the true position of the bony landmarks. The dimensions for the virtual markers were based on the dimensions from the non-reference foot. Kinematic data were recorded in 60Hz (frames per second). EMG data was collected using a Delsys wireless EMG signal detection system at 1200Hz [68] (Figure 3.3). Kinetic data was obtained from three Bertec force plates and one AMTI force plate at 1200Hz.

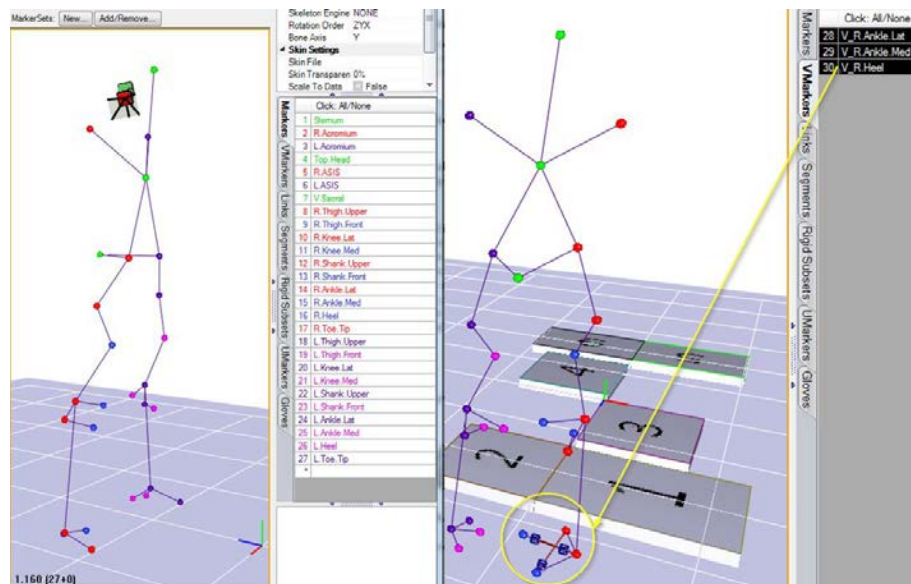


Figure 3.2 Markerset and virtual markers.



Figure 3.3 EMG detection system.

3.4 Modeling and Simulation

The walking simulations were generated using a musculoskeletal biomechanics simulation software (OpenSim v 3.3) [69]. A Primarily musculoskeletal model with two legs and a lumped torso segment that includes 23 degrees of freedom and 92 muscle-tendon actuators was used (Figure 3.4) [70]. It is possible to model ligaments in OpenSim by using the “Ligament” class. The inputs required by this class are: resting length—the length of the ligament at zero strain, the force length curve of the ligament as well as the physiological cross sectional area or PCSA which scales the force-length curve. The non-linear behavior of the ligament is modeled by the force-length curve by relating the ligament force to the normalized length of the ligament. As a result, no force is generated whenever the length of the ligament shortens beyond the resting length. Given that the ligament elasticity is not generally linear, it was necessary to use a ligament force-length curve. The equations found in [71] help to understand the necessary values and parameters to model the ligament and the force-length curve. These equations were based on the current ligament modeling techniques used in AnyBody Modeling System which is a musculoskeletal simulations software [72].

$$F = A + B\varepsilon + C\varepsilon^2 + D\varepsilon^4 \quad (3.4.1)$$

In equation (3.4.1) $A = 0$ and $B = k_{init}$ which is the initial stiffness and the stiffness where the stiffness is defined as $k = \frac{F_1}{\varepsilon * L_0}$ with L_0 being the resting length of the ligament. Obtaining the derivative of (3.4.1) with respect to strain ε yields equation (3.4.2). This allows to solve for the missing variables C and D (3.4.3).

$$\frac{dF}{d\varepsilon} = B + 2C\varepsilon + 4D\varepsilon^3 \quad (3.4.2)$$

$$\begin{bmatrix} \varepsilon_{nom}^2 & \varepsilon_{nom}^4 \\ 2\varepsilon_{nom} & 4\varepsilon_{nom}^3 \end{bmatrix} \times \begin{bmatrix} C \\ D \end{bmatrix} = \begin{bmatrix} F_{nom} - k_{init} * \varepsilon_{nom} \\ k_{nom} - k_{init} \end{bmatrix} \quad (3.4.3)$$

In order to describe the non-linearity behavior of the ligament, the following parameters are needed: the relative initial stiffness a_0 , and the relative stiffness at nominal strain a_1 . By introducing these parameters the initial stiffness k_{init} can be scaled by having it multiplied by a_0 and by the resting length of the ligament. In the same manner, the nominal stiffness k_{nom} is multiplied by the relative stiffness at nominal strain a_1 and the ligament resting length. Simply put, a_0 defines the slope of the force-length curve at the slack length of the ligament—at the beginning of the curve while it interpolates between zero slope and the linear part of the force-length curve. On the other hand, a_1 interpolates the curve closer to the yield region [72]. A PCSA force value for the anterior talofibular ligament was obtained from the extended OpenSim model of an ankle-foot complex described in [71]. The force-length curve of the anterior talofibular ligament is normalized by dividing every force value by this PCSA force. It is worth mentioning that the yield region of the characteristic ligament force-length curve was modeled as a constant factor.

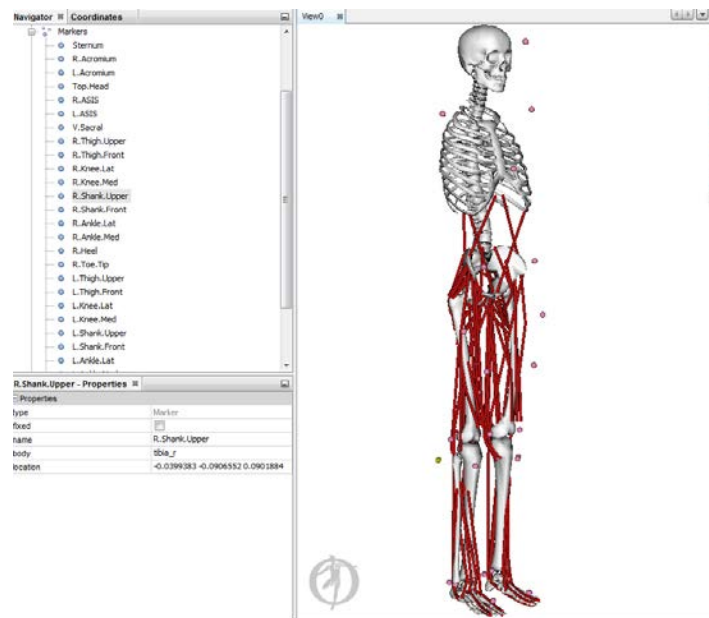


Figure 3.4 OpenSim lumped torso/lower limbs model.

The anterior talofibular ligament parameters were modeled based on literature from [72], [78]. The position of the talofibular ligament is illustrated in Figure 3.5 while (APPENDIX F) shows the “ligament class” used in the OpenSim model. Marker position data were imported into OpenSim to generate the walking simulations. The parameters of a full body musculoskeletal model were scaled using the OpenSim Scale Model tool to best fit the experimentally measured subject mass and marker positions [80]. The Inverse Kinematics tool was then used to calculate the limb segment positions and joint angles that reduced the difference between the experimental and virtual marker position data. The resultant kinematics and experimentally measured ground reaction forces were imported into the Computed Muscle Control (CMC) tool to calculate the muscle activations, lengths, associated muscles forces, and powers for all three experimental walking conditions.

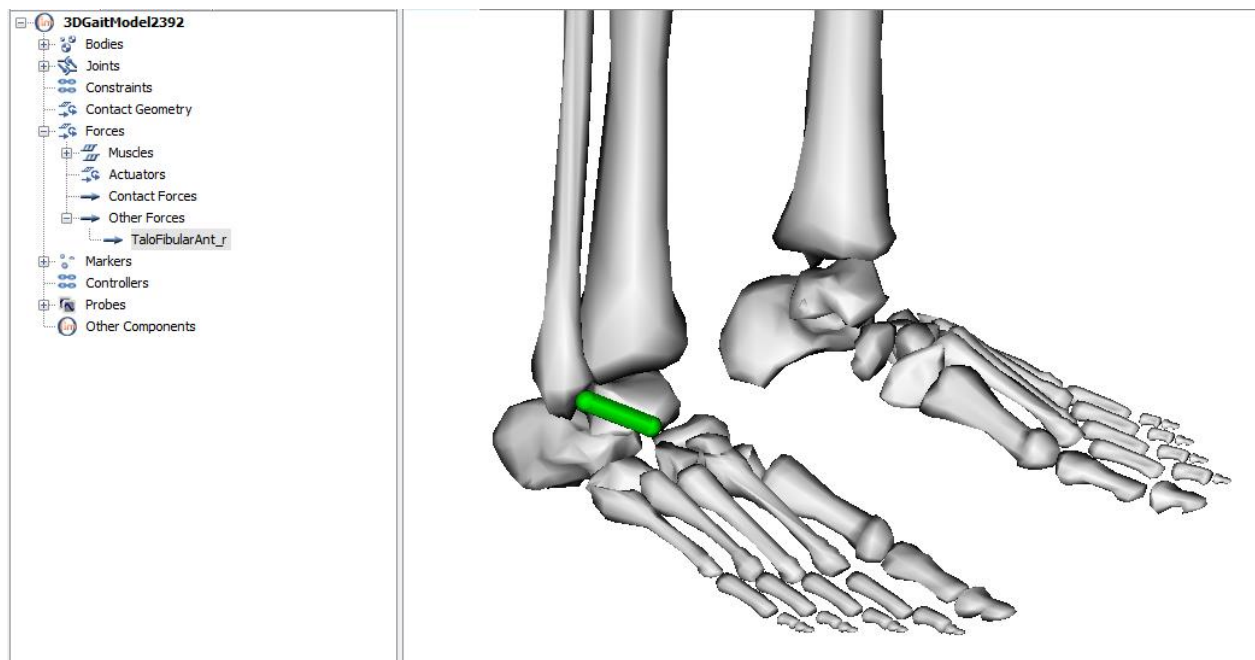


Figure 3.5 Talofibular ligament in OpenSim.

3.5 Method to Define the Beginning and End of Gait

The gait cycle used in this experiment is a modified gait cycle that includes an initial additional swing phase for the reference leg. This is to allow the Computed Muscle Control tool in OpenSim to settle down and minimize potential initial miscalculations of muscle activity. The start of the modified gait cycle takes into consideration heel strike of the non-reference leg, which is the beginning of the swing phase of the reference leg. This modified cycle continues until a second heel strike of the reference leg is achieved and this defines the end of the gait capture. Based on this definition of the modified gait cycle ([APPENDIX A](#)), trials of different time lengths were normalized as a percentage of gait capture and compared.

3.6 Data Analysis

3.6.1 Anterior Talofibular Ligament Forces

After running the CMC tool which produced muscle lengths, and associated muscles forces for all three experimental walking conditions, the forces exhibited by the anterior talofibular ligament, which is the ligament that is primarily affected in ankle sprains, were analyzed. This analysis was done by accessing the Analyze tool which used the CMC states as input in order to recreate the motion, but with an additional “Force Reporter” analysis which generated a *forces.sto file with the ligament forces throughout the gait simulation. Although the CMC simulations were only performed on 8 subjects, the kinematic data was still available for all 10 subjects which was enough data to plot the ligament since it is only a passive object.

3.6.2 Muscle Activity

In an effort to validate the forces displayed by the “Ligament” class, the collected EMG muscle activity was studied and compared against the OpenSim simulated muscle activity. For this, both the raw sampled EMG and muscle simulated data from OpenSim were filtered using a

zero phase lag sixth-order Butterworth digital filter with 6 Hz cutoff frequency and normalized to the highest value measured for the respective muscle while walking ([APPENDIX C](#)). The mean and the standard deviation were calculated from EMG data for all subjects and compared the corresponding muscle activations calculated by the CMC tool. Figure 3.6 shows an example of a CMC simulation in which muscles in red are active and muscles in blue are inactive. A one-way ANOVA with a Fishers Least Significant Difference (LSD) test was used to test for differences in the means of the groups.

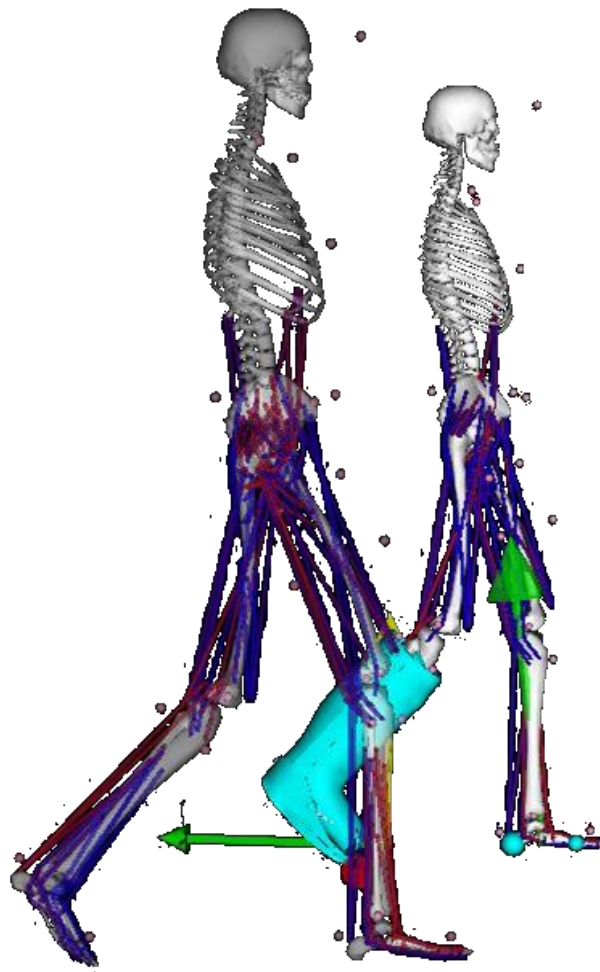


Figure 3.6 CMC simulation examples.

CHAPTER FOUR
RESULTS AND DISCUSSION

4.1 Anterior Talofibular Ligament Forces

As stated earlier, even though CMC simulations were not possible for 2 of the 10 subjects due to force-plate calibration issues, ligament forces were still obtained through OpenSim’s “Inverse Kinematic” and “Analyze” tools. All plots for the ATFL forces can be found in ([APPENDIX B](#)) The force response of the ATFL occurred during the initial swing phase and ended during the stance phase for all subjects. For Subject 1, the ATFL force response reached values of 41.1N, 5N, and 2.4N for the no boot, 0° PF/DF, and 20° PF/DF conditions respectively. Subject 5 reached values of 41N, 5.1N, and 2.5N for the no boot, 0° PF/DF, and 20° PF/DF conditions respectively. Subject 6 showed forces of 24N, 2.5N, and 0.5N for the no boot, 0° PF/DF, and 20° PF/DF conditions respectively. It was found that 7 out of 10 subjects showed forces for the “no boot” condition, but zero forces for both of the boot conditions (Table 4.1). These findings are further explored in the discussion section.

Table 4.1 Anterior Talofibular Ligament Peak Force

Anterior Talofibular Ligament Peak Force (N)			
Subject	No Boot	0° PF/DF	20° PF/DF
1	41.1	2.4	5
2	12.3	0	0
3	41.1	0	0
4	9.8	0	0
5	41.1	2.5	5.1
6	24	0.5	2.5
7	23.5	0	0
8	41.1	0	0
9	7.1	0	0
10	41.1	0	0

4.2 Muscle Activity

The EMG and CMC activations for walking with no boot as well as both of the boot conditions were qualitatively similar for the tibialis anterior and extensor digitorum longus for the 8 subjects studied. Reproducibility was not as achievable in terms of comparison for the peroneus longus in both of the boot conditions. The collected EMG activity for the tibialis anterior muscle averaged across subjects for the three conditions (no boot, boot at 0° PF/DF, and 20° PF/DF) was $0.420 \pm 0.137V$, $0.456 \pm 0.100V$, and $0.459 \pm 0.101V$, respectively (Table 4.2). The OpenSim simulated muscle activity for the tibialis anterior averaged across subjects for the three conditions were $0.322 \pm 0.071V$, $0.387 \pm 0.075V$, $0.400 \pm 0.082V$, respectively (Table 4.3). The mean EMG activity for the extensor digitorum longus for the three conditions was $0.322 \pm 0.095V$, $0.317 \pm 0.113V$, and $0.369 \pm 0.086V$, respectively (Table 4.2). The OpenSim simulated muscle activity for the extensor digitorum longus for the three conditions was $0.325 \pm 0.083V$, $0.383 \pm 0.083V$, and $0.386 \pm 0.086V$, respectively (Table 4.3). The mean EMG activity for the peroneus longus for the three conditions was $0.297 \pm 0.100V$, $0.256 \pm 0.128V$, and $0.290 \pm 0.118V$, respectively (Table 4.2). The OpenSim simulated muscle activity for the peroneus longus for the three conditions was $0.303 \pm 0.056V$, $0.379 \pm 0.116V$, and $0.350 \pm 0.066V$, respectively (Table 4.3). Figure 4.1 shows that the mean activity for the tibialis anterior actually increased when moving from the “no boot” to the “0° PF/DF” condition. The same increase behavior was observed in the tibialis anterior activity when moving to the “20° PF/DF” from the “0° PF/DF”. These occurrences were also applicable on the OpenSim simulated muscle activity, (Figure 4.1). The mean muscle activity for the extensor digitorum longus had a slight decrease in activity when moving from the “no boot” condition to the “0° PF/DF” condition in terms of the EMG collected data (Figure 4.2). This was not the case for the OpenSim activity since it actually increased when moving from “no boot” to

“0° PF/DF”. Just as in the case with the tibialis anterior, moving to “20° PF/DF” from the “0° PF/DF” showed an increase for the extensor digitorum longus in both the EMG and OpenSim muscle activations (Figure 4.2). Peroneus longus muscle activity appeared to be the muscle with the most variation present. In the case of the EMG collected data, this muscle showed a decrease in activity when moving from the “no boot” to “0° PF/DF” condition and then increased when moving to “20° PF/DF” (Figure 4.3). In the case of the OpenSim simulated data, the peroneus longus exhibited an increase in activity when moving from the “no boot” to “0° PF/DF” condition and then a decrease in activity when moving to “20° PF/DF” (Figure 4.3).

Table 4.2 EMG Muscle Activity (Volts)

EMG Muscle Activity									
Subject	No Boot			0° PF/DF			20° PF/DF		
	R. Tibialis Anterior	R. Digitorum Longus	R. Peroneus Longus	R. Tibialis Anterior	R. Digitorum Longus	R. Peroneus Longus	R. Tibialis Anterior	R. Digitorum Longus	R. Peroneus Longus
1	0.568	0.398	0.410	0.521	0.264	0.141	0.543	0.320	0.211
2	0.342	0.402	0.297	0.410	0.441	0.345	0.446	0.434	0.357
3	0.379	0.305	0.391	0.366	0.294	0.338	0.328	0.310	0.348
4	0.432	0.431	0.414	0.515	0.513	0.462	0.565	0.540	0.485
5	0.363	0.239	0.240	0.491	0.298	0.222	0.479	0.382	0.237
6	0.283	0.248	0.166	0.318	0.331	0.161	0.354	0.382	0.198
7	0.680	0.382	0.174	0.625	0.232	0.076	0.589	0.292	0.121
8	0.311	0.169	0.286	0.397	0.159	0.306	0.372	0.288	0.360
MEAN	0.420	0.322	0.297	0.456	0.317	0.256	0.459	0.369	0.290
SD	0.137	0.095	0.100	0.100	0.113	0.128	0.101	0.086	0.118

Table 4.3 OpenSim Muscle Activity (Volts)

OpenSim Muscle Activity									
Subject	No Boot			0° PF/DF			20° PF/DF		
	R. Tibialis Anterior	R. Digitorum Longus	R. Peroneus Longus	R. Tibialis Anterior	R. Digitorum Longus	R. Peroneus Longus	R. Tibialis Anterior	R. Digitorum Longus	R. Peroneus Longus
1	0.215	0.200	0.220	0.454	0.402	0.434	0.418	0.381	0.362
2	0.373	0.337	0.282	0.409	0.437	0.414	0.529	0.447	0.377
3	0.305	0.299	0.320	0.451	0.487	0.539	0.371	0.352	0.418
4	0.282	0.262	0.248	0.302	0.246	0.208	0.312	0.300	0.294
5	0.294	0.289	0.381	0.301	0.453	0.511	0.307	0.545	0.446
6	0.277	0.453	0.375	0.296	0.282	0.276	0.337	0.268	0.290
7	0.415	0.332	0.292	0.465	0.396	0.347	0.488	0.412	0.353
8	0.414	0.425	0.307	0.415	0.361	0.306	0.435	0.381	0.256
MEAN	0.322	0.325	0.303	0.387	0.383	0.379	0.400	0.386	0.350
SD	0.071	0.083	0.056	0.075	0.083	0.116	0.082	0.086	0.066

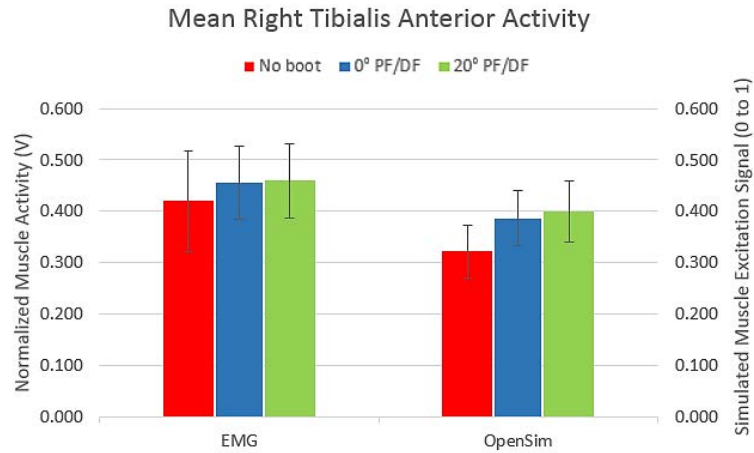


Figure 4.1 Mean right tibialis anterior activity.

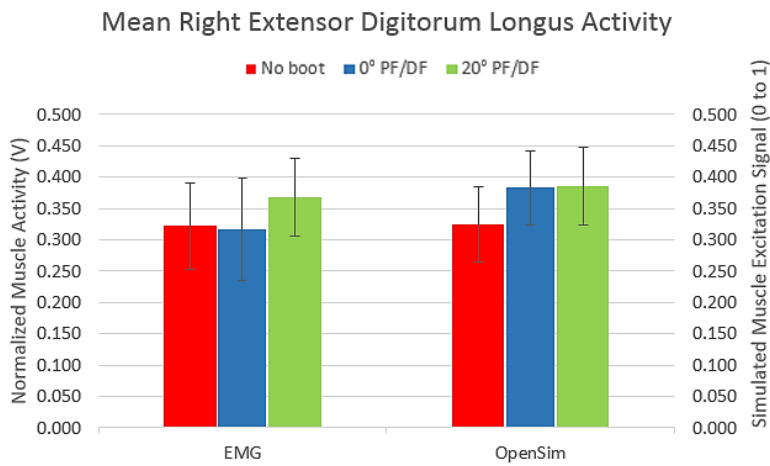


Figure 4.2 Mean right extensor digitorum longus activity.

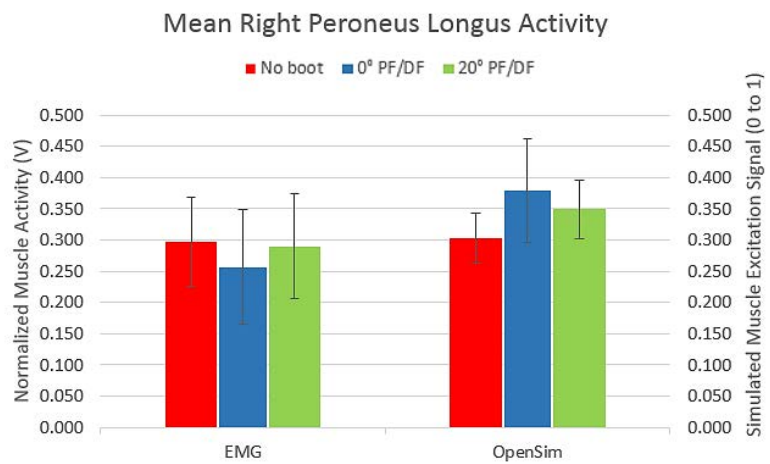


Figure 4.3 Mean right peroneus longus activity.

A one-way ANOVA was performed with an alpha level of 0.05. The independent variables/groups were the three experimental walking conditions and the three simulated walking conditions. The dependent variables were the EMG response and the OpenSim muscle excitation signal. The statistical analysis performed on the tibialis anterior showed that there was no overall significant difference between walking conditions when comparing EMG activity and simulated activity ($p = 0.071$). This p -value is marginally close to the 0.05 cutoff value. [APPENDIX D](#) shows the LSD multiple mean group comparisons for the TA and it is easy to observe that there was significant difference in the case of the “no-boot” condition comparison of the EMG and simulated muscle activity ($p = 0.05$). There was also no overall significant difference for the EDL statistical analysis when comparing experimental and simulated data for all three walking conditions ($p = 0.430$). Significant difference between collected and simulated muscle activity was encountered for the PL statistical analysis ($p = 0.035$). As expected, the simulated ligament forces decreased when wearing a rigid boot, and had a negligible increase with an articulated boot. As a whole, the ANOVA and LSD test on the extensor digitorum longus showed no significant difference. The ANOVA p -value for this muscle was ($p = 0.430$) while all of the LSD comparisons between EMG and simulated activities for all three walking conditions showed p -values well above ($p = 0.05$). High variability was encountered when comparing the collected and simulated muscle activities of the peroneus longus. The statistical analysis on this muscle showed an ANOVA ($p = 0.035$) and significantly low LSD p -values for the “rigid” and “articulated” conditions. This can be appreciated in [APPENDIX D](#).

4.3 Discussion

Multiple leg muscles play an important role during walking in order to achieve proper motor control, stability, and ground clearance. Ankle sprains are the most common injuries in the

athletic populations. These injuries are responsible for long-term disabilities, instability, and create additional issues such as muscle atrophy due to immobilization. The integrity of the affected ligaments during conservative and functional treatments of ankle sprains is not completely understood. The goal of this thesis was to create musculoskeletal dynamic simulations to validate the efficacy of functional articulated AFOs in providing muscle stimulation while simultaneously protecting the affected ligaments and promote a quick recovery. The results were divided in two sections. The first section illustrated the anterior ATFL forces in all three conditions. The following section compared EMG activity with simulated muscle activity. As expected, ligament forces diminished when the boot was applied and increased to a negligible degree when range of motion was allowed. This behavior demonstrates that the use of an articulated boot stimulates important musculature while maintaining injured ligament integrity. Nevertheless, unanticipated results were still present when studying ligament forces. Seven out of ten subjects did not exhibit ligament forces whatsoever for the “rigid (0° PF/DF)” and “articulated (20° PF/DF)” conditions. As far as muscle activity is concerned, the observed results indicate that general agreement was found when comparing experimental EMG activity, with OpenSim’s CMC activation patterns of the TA, EDL, and PL. This comparison was necessary in order to justify the ligament element used in the model. Before interpreting the meaning of such results it is important to reflect upon the assumptions and methodologies made in the study.

4.4 Methodological Issues

It is worth highlighting that the OpenSim musculoskeletal model had a lumped torso (no arms) and the lower extremities and segments included only 23 degrees of freedom and 92 muscle-tendon actuators. As a result, this model neglects the effects of forces and accelerations provoked by the arms throughout the gait cycle. However, the simulated muscle excitations in the simulation

are in agreement with the muscle activities found in the experimental collection. This provides confidence that the model excitations are representative of real life muscle activations. Additionally, every motion capture experiment is only as good as the initial calibration of the equipment. This of course extends to the accuracy in regards to marker and electrode placement. Every effort was made in placing EMG electrodes as precise as possible on the subjects' lower limbs. However, because of anatomical variability, there was potential muscle crosstalk. The case of systemic influenced effects is also possible because subjects were allowed to walk at their own comfortable speed. Lastly, it is also important to consider the size of the study. The decision to collect data from ten subjects was made by bearing in mind the time required to collect and post-process the data as well as generating computed muscle control simulations. The recruitment of ten subjects was deemed suitable mainly due to the prolonged processes of the experiment.

4.5 Interpretation of Results

The results of the anterior talofibular ligament forces have notable unexpected values. Seven out of ten subjects did not show any stretching of the ligament in both of the boot conditions. It is important to recall that—as mentioned in the *Modeling and Simulation* section—the yield region of the characteristic ligament force-length curve was modeled as a constant factor. This force-length curve constant factor and the PCSA values can be a limitation since—unlike the slack length of the ligament—they do not automatically adjust during the scaling process. This limitation would indicate that subject specific values are needed for more accurate results. A reduction in ATFL force was expected, but not to the extent of obtaining zero force. For this reason, the angles of the ankle joint were investigated in hopes of deciphering what caused these values. It is worth emphasizing that the ATFL typically fails when subjected to extreme inversion about the ankle joint and at forces of $245 \pm 40\text{N}$ [47]. Regular walking does not approach such high values.

Subject 2, shown in Figure 4.4 was one of the seven subjects that did not exhibit ligament stretching for the boot conditions. This subject was selected in order to compare dorsiflexion and plantarflexion angles with the ATFL ligament forces to further understand the values.

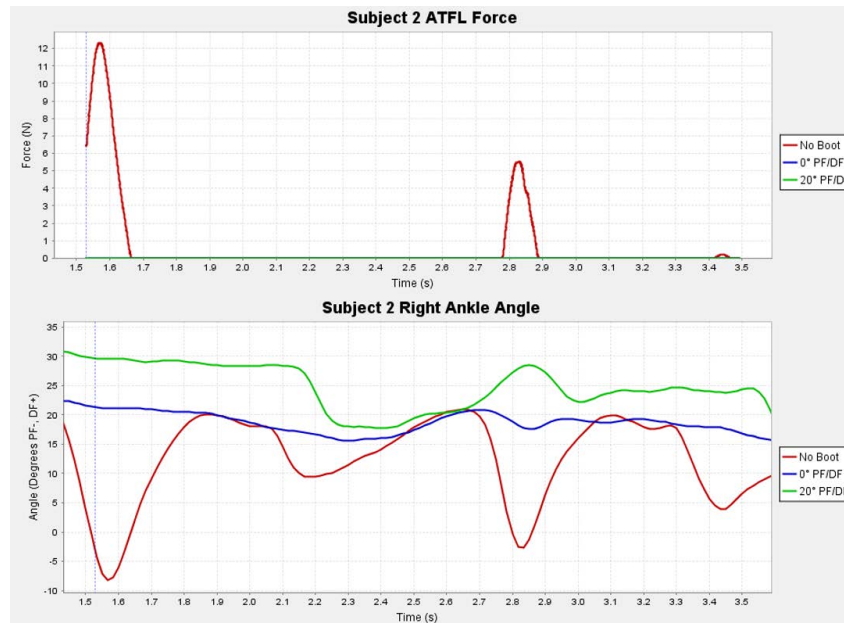


Figure 4.4 Subject 2 ATFL forces vs ankle joint angles.

In the gait cycle, the foot usually enters a relaxed plantarflexion stage immediately after the toe-off phase. The foot is then lifted to clear the ground right before heel-impact. By comparing the peaks of the ATFL forces and the wells of the plantarflexion angles it is evident that for both of the boot conditions, subject 2 was unable to relax the ankle so as to allow plantarflexion during the swing phase. This led to the conclusion that the design of the boot was affecting gait characteristics. The articulated ankle joint in the boot happens to allow plantarflexion, but this can also be limited in some cases. This is because the articulated joint is not a frictionless joint and as soon as dorsiflexion is introduced the boot actually keeps the foot in that position throughout the gait cycle. In other words, a large amount of force during the toe-off phase is needed in order to plantar-flex and observe ligament stretching. In summary, because of the friction encountered in

the articulated boot joint; seven out ten subjects showed signs of actually having their foot sustained by the boot in a neutral position during the swing phase even though plantarflexion was allowed to 20°. The kinematics showing natural plantarflexion during swing phase by Subject 2 are observed in Figure 4.5, while Figure 4.6 shows a lack of plantarflexion as a result of the boot carrying the foot in a dorsi-flexed position. An additional factor that may contribute to extreme dorsi-flexed angles observed in the figures is the methodology employed for the placement of reflective markers. Subject 2 had shorter lower limbs and the marker location of the shank had to be placed on the boot itself. Virtual markers were created to account for the ankle positions, but this was not the case for the shank. It is possible that the location of the marker could have an effect during the scaling process. Figure 4.7 shows the location of the marker for the shank placed on the surface of the boot.

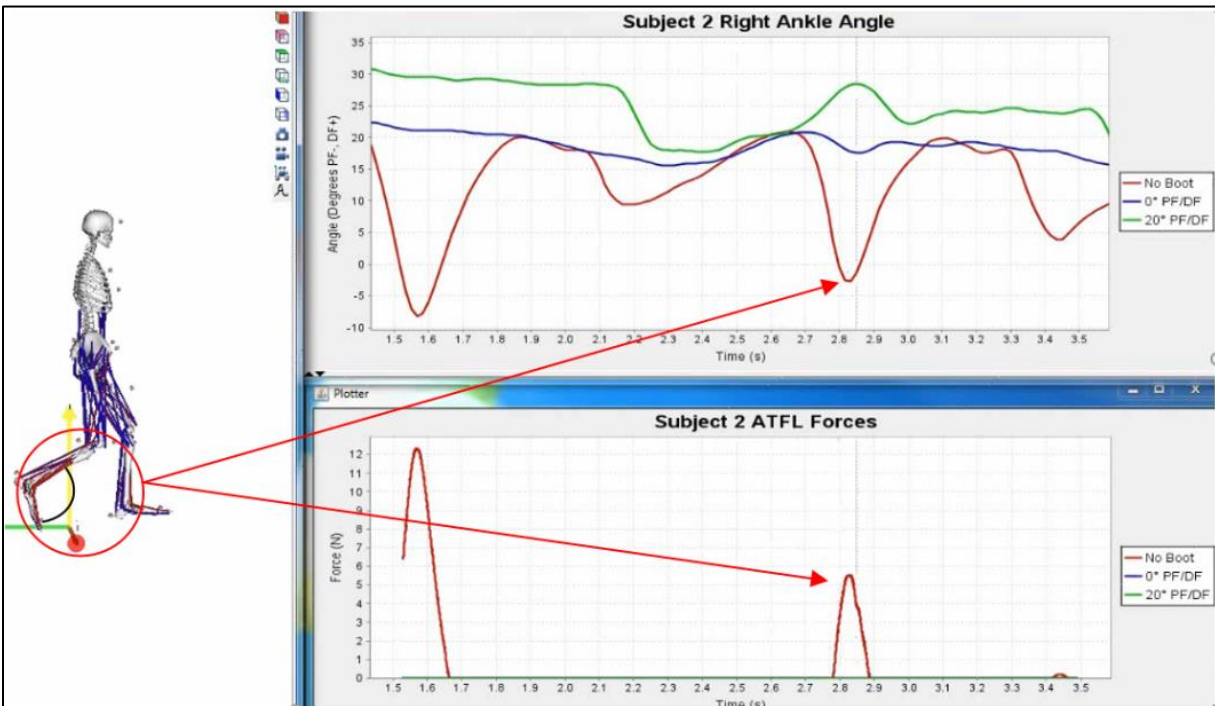


Figure 4.5 Subject 2 CMC no boot condition simulation.

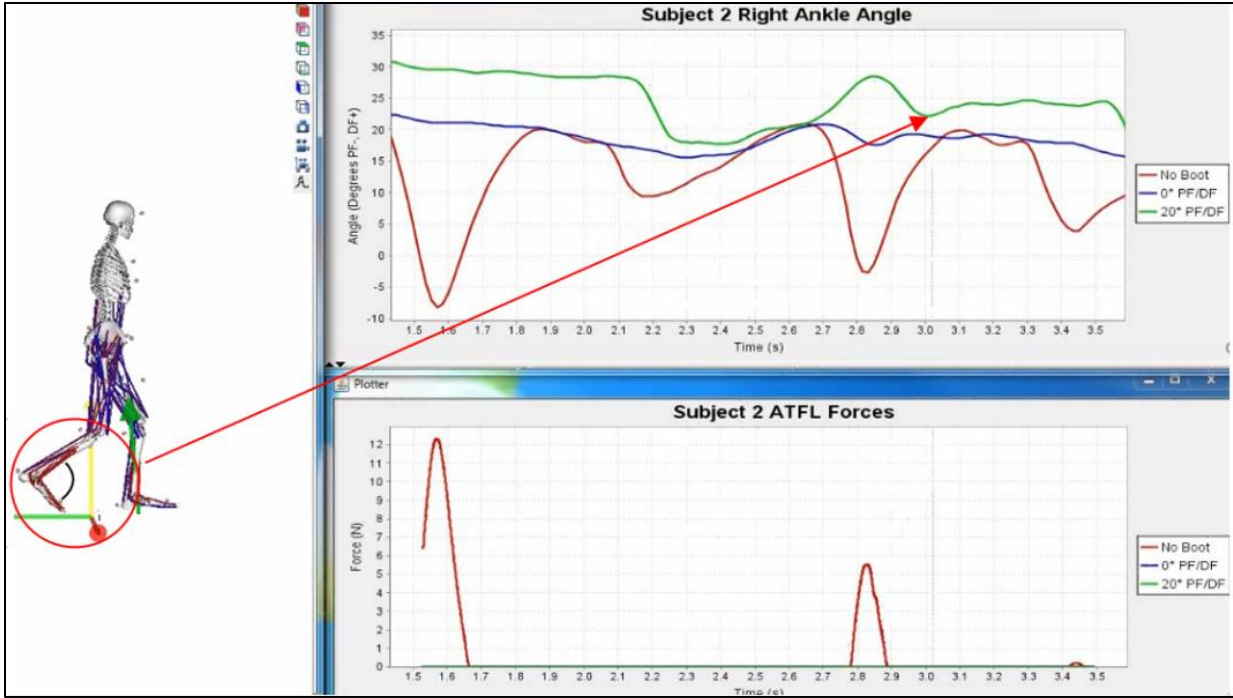


Figure 4.6 Subject 2 CMC articulated boot condition simulation.



Figure 4.7 Subject 2 marker placement on boot.

The lack of plantarflexion and zero ligament force occurrence actually links to the variability observed in the statistical analysis of the peroneus longus muscle activation comparison of EMG and OpenSim. The results of the statistical analysis of the TA and EDL showed that the collected EMG activity and OpenSim simulated muscle excitations are in agreement with each other. In the case of the PL, the “no boot” conditions of the experimental EMG data and the computed muscle control excitations did not show a significant difference ($p = 0.619$). However, there was significant difference encountered in both, the rigid 0° PF/DF and the 20° PF/DF conditions with ($p = 0.011$) and ($p = 0.030$), respectively. A study conducted by Konradsen and Hojsgaard [9] provided indirect evidence of a corrective mechanism occurring due to contraction of the peroneal muscles if the ankle joint inversion is perceived to be too great in transitioning from mid-swing to terminal swing phase of gait. During this experiment, they observed a reduction in peroneal muscle activation after the application of an ankle support that held the ankle joint in a neutral position of inversion/eversion. The authors concluded that the reduced peroneal muscle activation was the result of a reduced need for eversion corrections. In retrospect, the EMG PL muscle activity for both of the boot conditions in Figure 4.3 shows a decrease in muscle recruitment. This agrees with the findings of Konradsen and Hojsgaard and correlates to the absence of ATFL forces due to stretching. Another interesting thing to point out is that muscle activity of the TA and EDL appeared to actually increase whenever the boots were used. AFOs tend to minimize plantarflexion, inversion and eversion, but it is also conceivable that while activity of supported muscles decreases, activity in antagonistic muscles sometimes increases. Possible explanations can be that the muscles are trying to compensate for the extra weight added imposed on the leg. For instance, Diez et al [81] and Cerny et al [82], encountered higher EMG activity excitations of proximal musculature of the leg when subjects used a knee brace that

restricted knee extension. Similarly, studies conducted by Jansen et al [83] and Bulthaupt et al [84] showed that proximal muscle activity increased together with a decrease of activity of the supported wrist extensor muscles in patients who wore wrist orthoses. With that said, another possible factor that contributed to the increase activity of the TA and EDL in the boot conditions may be due to the fact that the subjects in this study were all healthy volunteers with nonparetic muscles. Additionally, these subjects may have recruited the TA and EDL in isometric contractions which as mentioned earlier, occur when muscles statically resist or oppose forces acting on a limb about a joint and do not involve lengthening or shortening of muscles at all [41]. Finally, it can be inferred from the results that the use of an articulated walker showed a slightly higher muscle activity which can help stimulate the muscles throughout functional treatment of ankle sprains. The ATFL forces showed a decrease with the rigid boot condition and an increase of these forces when range of motion was introduced. The force increase between the “rigid” and “articulated” boot conditions was only of around 2.5N compared to the force difference from the “no boot” and “rigid boot” condition that ranged between 24-41.7N. These forces are nowhere close to the failure forces of $245 \pm 40\text{N}$ [47]. However, it is important to keep in mind that although the results showed that muscle stimulation and ligament integrity was achieved, the results of studies performed on healthy subjects cannot be extrapolated to patients with ankle instabilities without proper attention. It is expected that a different muscle reaction response with potentially larger variety can occur in patients with paretic musculature.

CHAPTER FIVE

CONCLUSIONS AND RECOMMENDATIONS

5.1 Conclusions

This study took into consideration the importance of functional therapy as a permissive early treatment for severe ankle sprains. The intention was to present a new approach for studying ankle sprains and provide new insights with the potential to accelerate ankle sprain rehabilitation. In regards to ankle sprains, the integrity of the injured ligaments during conservative and functional treatments is not fully understood. The anterior talofibular ligament is usually the first ligament to be injured during an inversion sprain. Immobilization of this ligament is crucial in terms of recovery. However, it is essential to consider an alternative type of treatment often referred to as “functional therapy” in which the integrity of the ligament is protected while still allowing muscular stimulation. This type of treatment aims to address some of the side effects of long periods of inactivity such as muscle atrophy and functional instability of the ankle joint. The idea for this thesis was to validate the use of an articulated AFO and its ability to promote muscle activation while maintaining integrity on the anterior talofibular ligament. Three walking conditions were presented to compare the results (regular walking, walking with a rigid boot, and walking with an articulated boot). The investigation was carried out through the use of musculoskeletal dynamic simulations. The results were divided into two sections. First, the forces encountered in the ATFL during the gait trials were examined. Then, the muscle activity of the TA, EDL, and PL for the three walking conditions was studied and compared against the simulated excitations from OpenSim. It is important to highlight that in the case of the forces experienced by the ATFL, 7 out of 10 subjects notably displayed values of zero force for the boot conditions. A reduction of ligament stretching was expected, but not to the point of obtaining zero forces. It was

established that because of the friction encountered in the articulated boot joint; subjects showed signs of actually having their foot in a dorsi-flexed position during the swing phase resulting in no plantarflexion and therefore no stretching of the ligament. When comparing EMG with OpenSim's CMC activation patterns, the PL was the only muscle with significant difference encountered in both, the rigid and articulated boot conditions with ($p = 0.011$) and ($p = 0.030$), respectively. Nevertheless, general agreement was found for the TA and EDL with overall ANOVA p -values of 0.071 and 0.430, respectively. This provided confidence in the simulation and indicated that superior results may be achieved with proper refinements to the ATFL parameters. Literature seems to agree that concerning effectiveness, functional treatment currently seems a more appropriate style of therapy for ankle sprains. The research performed in this study indicates that the use of articulated ankle foot orthoses does in fact stimulate important muscle activity necessary for proper motor control while in turn maintaining the ATFL forces at a minimal. Altogether, the results demonstrated the importance of musculoskeletal dynamic simulations and how they may serve as a tool to uncover the biomechanical causes of movement abnormalities, and help design improved treatments.

5.2 Recommendations for Future Studies

The experiments done in this thesis pertain primarily with grade III ankle sprains and the use of a rigid AFO. In terms of grade I and II ankle sprains, the use of bracing and taping is typically recommended as part of rehabilitation. Similar studies to the one performed in this work can be carried out with the use of non-rigid ankle sprain braces given that evidence to support the effectiveness of applying ankle braces during the acute and subacute phases of ankle rehabilitation is still needed [85].

REFERENCES

REFERENCES

- [1] VEENEMA, K. R., “Ankle sprain: Primary care evaluation and rehabilitation,” *J. Musculoskelet. Med.*, vol. 17, no. 9, 2000, pp. 563–563.
- [2] Reid, D. C., “Sports injury, assessment and rehabilitation,” *Med. Sci. Sports Exerc.*, vol. 25, no. 10, 1993, p. i.
- [3] Beynnon, B. D., Renström, P. A., Haugh, L., Uh, B. S., and Barker, H., “A prospective, randomized clinical investigation of the treatment of first-time ankle sprains,” *Am. J. Sports Med.*, vol. 34, no. 9, 2006, pp. 1401–1412.
- [4] DiFiori, J. P., “Diagnosis and management of selected sportsrelated injuries,” *Pri-Med Lect.*, 2003, pp. 365–378.
- [5] Kerkhoffs, G. M., Rowe, B. H., Assendelft, W. J., Kelly, K. D., Struijs, P. A., and van Dijk, C. N., “Immobilisation for acute ankle sprain,” *Arch. Orthop. Trauma Surg.*, vol. 121, no. 8, 2001, pp. 462–471.
- [6] Cifu, D. X., *Braddom’s physical medicine and rehabilitation*. Elsevier Health Sciences, 2015.
- [7] Cohen, R. S. and Balcom, T. A., “Current treatment options for ankle injuries: lateral ankle sprain, Achilles tendonitis, and Achilles rupture,” *Curr. Sports Med. Rep.*, vol. 2, no. 5, 2003, pp. 251–254.
- [8] Delahunt, E., Monaghan, K., and Caulfield, B., “Altered neuromuscular control and ankle joint kinematics during walking in subjects with functional instability of the ankle joint,” *Am. J. Sports Med.*, vol. 34, no. 12, 2006, pp. 1970–1976.
- [9] Konradsen, L. and Højsgaard, C., “Pre-heel-strike peroneal muscle activity during walking and running with and without an external ankle support,” *Scand. J. Med. Sci. Sports*, vol. 3, no. 2, 1993, pp. 99–103.
- [10] Geboers, J. F., Drost, M. R., Spaans, F., Kuipers, H., and Seelen, H. A., “Immediate and long-term effects of ankle-foot orthosis on muscle activity during walking: a randomized study of patients with unilateral foot drop,” *Arch. Phys. Med. Rehabil.*, vol. 83, no. 2, 2002, pp. 240–245.
- [11] Verhagen, E., Van der Beek, A., Twisk, J., Bouter, L., Bahr, R., and Van Mechelen, W., “The effect of a proprioceptive balance board training program for the prevention of ankle sprains a prospective controlled trial,” *Am. J. Sports Med.*, vol. 32, no. 6, 2004, pp. 1385–1393.

- [12] Banks, A., Downey, M., Martin, D., and Miller, S., *Foot and ankle surgery*. Philadelphia: Lipincott Williams & Wilkins, 2001.
- [13] Palmieri-Smith, R. M., Ty Hopkins, J., and Brown, T. N., “Peroneal activation deficits in persons with functional ankle instability,” *Am. J. Sports Med.*, vol. 37, no. 5, 2009, pp. 982–988.
- [14] Waterman, B. R., Owens, B. D., Davey, S., Zacchilli, M. A., and Belmont, P. J., “The epidemiology of ankle sprains in the United States,” *J Bone Jt. Surg Am*, vol. 92, no. 13, 2010, pp. 2279–2284.
- [15] Robbins, S. and Waked, E., “Factors associated with ankle injuries,” *Sports Med.*, vol. 25, no. 1, 1998, pp. 63–72.
- [16] Yeung, M. S., Chan, K. M., So, C. H., and Yuan, W. Y., “An epidemiological survey on ankle sprain,” *Br. J. Sports Med.*, vol. 28, no. 2, Jun. 1994, pp. 112–116.
- [17] Nussbaum, M. C. and others, *Aristotle’s De Motu Animalium: Text with translation, commentary, and interpretive essays*. Princeton University Press, 1985.
- [18] Goss, C. M., “On movement of muscles by Galen of Pergamon,” *Dev. Dyn.*, vol. 123, no. 1, 1968, pp. 1–25.
- [19] Keele, K. D., *Leonardo da Vinci’s Elements of the Science of Man*. Academic Press, 2014.
- [20] Andry, N., *L’Orthopédie ou l’art de prévenir et de corriger dans les enfans, les difformités du corps...* Chez La Veuve Alix, 1741.
- [21] Joseph, A., *Practical Podiatry*. First Institute of Podiatry, 1918.
- [22] Kirby, K. A., “Evolution of foot orthoses in sports,” in *Athletic Footwear and Orthoses in Sports Medicine*, Springer, 2010, pp. 19–35.
- [23] Isakov, E., Mizrahi, J., Onna, I., and Susak, Z., “The control of genu recurvatum by combining the Swedish knee-cage and an ankle-foot brace,” *Disabil. Rehabil.*, vol. 14, no. 4, Dec. 1992, pp. 187–191.
- [24] Chen, C. L., Yeung, K. T., Wang, C. H., Chu, H. T., and Yeh, C. Y., “Anterior ankle-foot orthosis effects on postural stability in hemiplegic patients,” *Arch. Phys. Med. Rehabil.*, vol. 80, no. 12, Dec. 1999, pp. 1587–1592.
- [25] Burdett, R. G., Borello-France, D., Blatchly, C., and Potter, C., “Gait comparison of subjects with hemiplegia walking unbraced, with ankle-foot orthosis, and with Air-Stirrup brace,” *Phys. Ther.*, vol. 68, no. 8, Aug. 1988, pp. 1197–1203.

- [26] Ounpuu, S., Bell, K. J., Davis, R. B., and DeLuca, P. A., “An evaluation of the posterior leaf spring orthosis using joint kinematics and kinetics,” *J. Pediatr. Orthop.*, vol. 16, no. 3, Jun. 1996, pp. 378–384.
- [27] Mulroy, S. J., Eberly, V. J., Gronely, J. K., Weiss, W., and Newsam, C. J., “Effect of AFO design on walking after stroke: impact of ankle plantar flexion contracture,” *Prosthet. Orthot. Int.*, vol. 34, no. 3, Sep. 2010, pp. 277–292.
- [28] Malliaropoulos, N., Ntessalen, M., Papacostas, E., Giuseppe Longo, U., and Maffulli, N., “Reinjury after acute lateral ankle sprains in elite track and field athletes,” *Am. J. Sports Med.*, vol. 37, no. 9, 2009, pp. 1755–1761.
- [29] Inman, V. T., *The joints of the ankle*. Williams & Wilkins, 1976.
- [30] Dubin, J. C., Comeau, D., McClelland, R. I., Dubin, R. A., and Ferrel, E., “Lateral and syndesmotric ankle sprain injuries: a narrative literature review,” *J. Chiropr. Med.*, vol. 10, no. 3, 2011, pp. 204–219.
- [31] Sarrafian, S. K., “Biomechanics of the subtalar joint complex,” *Clin. Orthop.*, vol. 290, 1993, pp. 17–26.
- [32] Scott, W. N., *The knee*, vol. 2. Mosby-Year Book, 1994.
- [33] Clanton, T. O. and Paul, P., “Syndesmosis injuries in athletes,” *Foot Ankle Clin.*, vol. 7, no. 3, 2002, pp. 529–549.
- [34] Kennedy, M. A., Sama, A. E., and Sigman, M., “Tibiofibular syndesmosis and ossification. Case report: sequelae of ankle sprain in an adolescent football player,” *J. Emerg. Med.*, vol. 18, no. 2, 2000, pp. 233–240.
- [35] Mei-Dan, O., Kots, E., Barchilon, V., Massarwe, S., Nyska, M., and Mann, G., “A dynamic ultrasound examination for the diagnosis of ankle syndesmotric injury in professional athletes a preliminary study,” *Am. J. Sports Med.*, vol. 37, no. 5, 2009, pp. 1009–1016.
- [36] Safran, M. R., Zachazewski, J. E., Benedetti, R. S., Bartolozzi 3rd, A., and Mandelbaum, R., “Lateral ankle sprains: a comprehensive review part 2: treatment and rehabilitation with an emphasis on the athlete,” *Med. Sci. Sports Exerc.*, vol. 31, no. 7 Suppl, 1999, pp. S438–47.
- [37] Hertel, J., Denegar, C. R., Monroe, M. M., and Stokes, W. L., “Talocrural and subtalar joint instability after lateral ankle sprain,” *Med. Sci. Sports Exerc.*, vol. 31, no. 11, 1999, pp. 1501–1508.
- [38] Burks, R. T. and Morgan, J., “Anatomy of the lateral ankle ligaments,” *Am. J. Sports Med.*, vol. 22, no. 1, 1994, pp. 72–77.

- [39] Beumer, A., van Hemert, W. L., Swierstra, B. A., Jasper, L. E., and Belkoff, S. M., “A biomechanical evaluation of the tibiofibular and tibiotalar ligaments of the ankle,” *Foot Ankle Int.*, vol. 24, no. 5, 2003, pp. 426–429.
- [40] Santilli, V. *et al.*, “Peroneus Longus Muscle Activation Pattern During Gait Cycle in Athletes Affected by Functional Ankle Instability A Surface Electromyographic Study,” *Am. J. Sports Med.*, vol. 33, no. 8, 2005, pp. 1183–1187.
- [41] Haff, G. G. and Triplett, N. T., *Essentials of Strength Training and Conditioning 4th Edition*. Human kinetics, 2015.
- [42] Dalley, A. F. and Moore, K. L., *Clinically oriented anatomy*. Lippincott Williams and Wilkins, Baltimore, MD, 1999.
- [43] Konradsen, L., Olesen, S., and Hansen, H. M., “Ankle sensorimotor control and eversion strength after acute ankle inversion injuries,” *Am. J. Sports Med.*, vol. 26, no. 1, 1998, pp. 72–77.
- [44] Wilkerson, G. B., Pinerola, J. J., and Caturano, R. W., “Invertor vs. evertor peak torque and power deficiencies associated with lateral ankle ligament injury,” *J. Orthop. Sports Phys. Ther.*, vol. 26, no. 2, 1997, pp. 78–86.
- [45] Marcus Hollis, J., Dale Blasier, R., and Flahiff, C. M., “Simulated lateral ankle ligamentous injury: change in ankle stability,” *Am. J. Sports Med.*, vol. 23, no. 6, 1995, pp. 672–677.
- [46] Andersen, T. E., Floerenes, T. W., Arnason, A., and Bahr, R., “Video analysis of the mechanisms for ankle injuries in football,” *Am. J. Sports Med.*, vol. 32, no. 1_suppl, 2004, p. 69S–79S.
- [47] Panagiotakis, E., Mok, K.-M., Fong, D. T.-P., and Bull, A. M. J., “Biomechanical analysis of ankle ligamentous sprain injury cases from televised basketball games: Understanding when, how and why ligament failure occurs,” *J. Sci. Med. Sport*, May 2017.
- [48] Uys, H. D. and Rijke, A. M., “Clinical Association of Acute Lateral Ankle Sprain with Syndesmotomic Involvement A Stress Radiography and Magnetic Resonance Imaging Study,” *Am. J. Sports Med.*, vol. 30, no. 6, 2002, pp. 816–822.
- [49] Wright, R. W., Barile, R. J., Surprenant, D. A., and Matava, M. J., “Ankle syndesmosis sprains in national hockey league players,” *Am. J. Sports Med.*, vol. 32, no. 8, 2004, pp. 1941–1945.
- [50] Inman, V. T., Ralston, H. J., and Todd, F., *Human walking*. Williams & Wilkins, 1981.
- [51] Perry, J., Davids, J. R., and others, “Gait analysis: normal and pathological function.,” *J. Pediatr. Orthop.*, vol. 12, no. 6, 1992, p. 815.

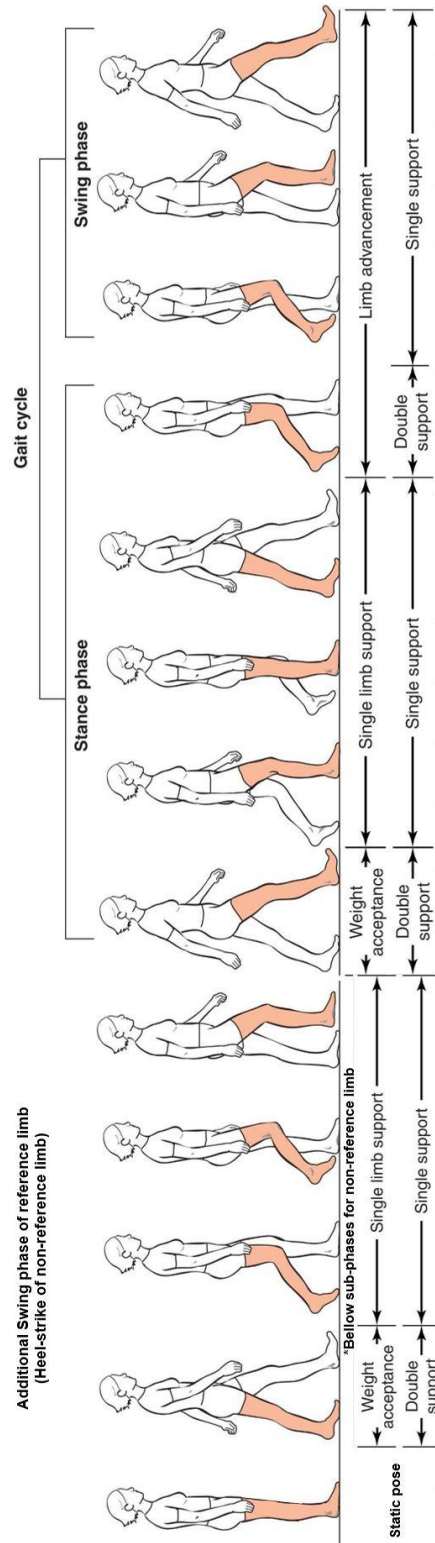
- [52] OpenStax CNX, “Types of Body Movements,” *OpenStax CNX*, 04-Jun-2013. [Online]. Available: <https://cnx.org/contents/qCnsYyus@3/Types-of-Body-Movements>. [Accessed: 16-May-2017].
- [53] Levangie, P. K. and Norkin, C. C., *Joint structure and function: a comprehensive analysis*. FA Davis, 2011.
- [54] Sutherland, D. H., “The evolution of clinical gait analysis: Part II Kinematics,” *Gait Posture*, vol. 16, no. 2, 2002, pp. 159–179.
- [55] Robertson, D. G. E., *Introduction to biomechanics for human motion analysis*. Waterloo Biomechanics, 1997.
- [56] O’Malley, M. and de Paor, D. L. A., “Kinematic analysis of human walking gait using digital image processing,” *Med. Biol. Eng. Comput.*, vol. 31, no. 4, 1993, pp. 392–398.
- [57] Syngellakis, S., Arnold, M., and Rassoulia, H., “Assessment of the non-linear behaviour of plastic ankle foot orthoses by the finite element method,” *Proc. Inst. Mech. Eng. [H]*, vol. 214, no. 5, 2000, pp. 527–539.
- [58] Olney, S., “Gait,” *Levangie P Norkin CC Jt. Struct. Funct. Compr. Anal. Fourth Ed Philadelphia FA Davis*, 2005, pp. 517–568.
- [59] Ayyappa, E., “Normal Human Locomotion, Part 1: Basic Concepts and Terminology,” *JPO J. Prosthet. Orthot.*, vol. 9, no. 1, 1997, pp. 10–17.
- [60] De Jalon, J. G. and Bayo, E., *Kinematic and dynamic simulation of multibody systems: the real-time challenge*. Springer Science & Business Media, 2012.
- [61] Parker, K., Naumann, S., Cleghorn, W., Belbin, G., and Slack, M., “Analysis and design modification of a paediatric ankle-foot orthosis,” *J. Rehabil. Res. Dev.*, vol. 33, 1996, p. 214.
- [62] Sutherland, D. H., “The evolution of clinical gait analysis part I: kinesiological EMG,” *Gait Posture*, vol. 14, no. 1, 2001, pp. 61–70.
- [63] Kamen, G. and Kinesiology, E., “Research methods in biomechanics,” *Champaign IL Hum. Kinet. Publ*, 2004.
- [64] Zhang, S., Clowers, K. G., and Powell, D., “Ground reaction force and 3D biomechanical characteristics of walking in short-leg walkers,” *Gait Posture*, vol. 24, no. 4, 2006, pp. 487–492.
- [65] Keefer, M., King, J., Powell, D., Krusenklau, J. H., and Zhang, S., “Effects of modified short-leg walkers on ground reaction force characteristics,” *Clin. Biomech.*, vol. 23, no. 9, 2008, pp. 1172–1177.

- [66] Kadel, N. J., Segal, A., Orendurff, M., Shofer, J., and Sangeorzan, B., “The efficacy of two methods of ankle immobilization in reducing gastrocnemius, soleus, and peroneal muscle activity during stance phase of gait,” *Foot Ankle Int.*, vol. 25, no. 6, 2004, pp. 406–409.
- [67] Fröberg, Å., Komi, P., Ishikawa, M., Movin, T., and Arndt, A., “Force in the achilles tendon during walking with ankle foot orthosis,” *Am. J. Sports Med.*, vol. 37, no. 6, 2009, pp. 1200–1207.
- [68] “Trigno Lab | Wireless EMG System.” [Online]. Available: <http://www.delsys.com/products/wireless-emg/trigno-lab/>. [Accessed: 25-Nov-2017].
- [69] Delp, S. L. *et al.*, “OpenSim: open-source software to create and analyze dynamic simulations of movement,” *IEEE Trans. Biomed. Eng.*, vol. 54, no. 11, Nov. 2007, pp. 1940–1950.
- [70] Delp, S. L., Loan, J. P., Hoy, M. G., Zajac, F. E., Topp, E. L., and Rosen, J. M., “An interactive graphics-based model of the lower extremity to study orthopaedic surgical procedures,” *IEEE Trans. Biomed. Eng.*, vol. 37, no. 8, Aug. 1990, pp. 757–767.
- [71] Silveira, A. C. P. da, “Extended Biomechanical Model of the Ankle-Foot Complex: Incorporation of Muscles and Ligaments,” 2015.
- [72] “Anybody Tutorials - Lesson7: Ligaments.” *A/S AnyBody Technology*. [Online]. Available: http://www.anybodytech.com/fileadmin/AnyBody/Docs/Tutorials/chap5_Muscle_modeling/lesson7.html. [Accessed: 26-Nov-2017].
- [73] Funk, J. R., Hall, G. W., Crandall, J. R., and Pilkey, W. D., “Linear and quasi-linear viscoelastic characterization of ankle ligaments,” *J. Biomech. Eng.*, vol. 122, no. 1, Feb. 2000, pp. 15–22.
- [74] Mengiardi, B. *et al.*, “Spring ligament complex: MR imaging-anatomic correlation and findings in asymptomatic subjects,” *Radiology*, vol. 237, no. 1, Oct. 2005, pp. 242–249.
- [75] Carmo, C. C. M. do, Melão, L. I. F. de A., Weber, M. F. V. de L., Trudell, D., and Resnick, D., “Anatomical features of plantar aponeurosis: cadaveric study using ultrasonography and magnetic resonance imaging,” *Skeletal Radiol.*, vol. 37, no. 10, Oct. 2008, pp. 929–935.
- [76] Patil, V., Ebraheim, N. A., Frogameni, A., and Liu, J., “Morphometric Dimensions of the Calcaneonavicular (Spring) Ligament,” *Foot Ankle Int.*, vol. 28, no. 8, Aug. 2007, pp. 927–932.
- [77] Rule, J., Yao, L., and Seeger, L. L., “Spring ligament of the ankle: Normal MR anatomy - eScholarship,” vol. 161, no. 6, Jan. 1993, pp. 1241–1244.
- [78] Stagni, R., Leardini, A., and Ensini, A., “Ligament fibre recruitment at the human ankle joint complex in passive flexion,” *J. Biomech.*, vol. 37, no. 12, Dec. 2004, pp. 1823–1829.

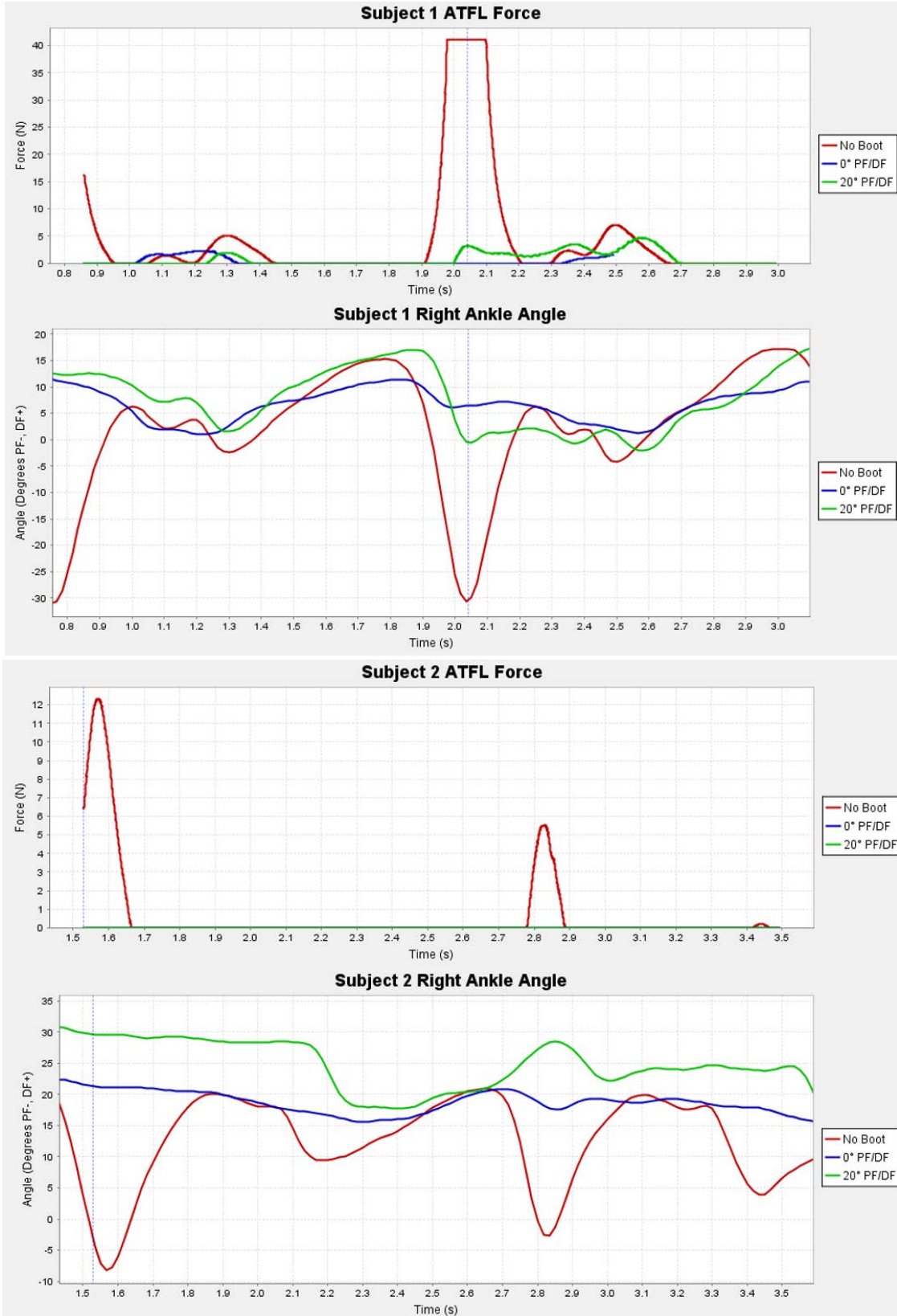
- [79] Golanó, P. *et al.*, “Anatomy of the ankle ligaments: a pictorial essay,” *Knee Surg. Sports Traumatol. Arthrosc.*, vol. 18, no. 5, May 2010, pp. 557–569.
- [80] Hamner, S. R., Seth, A., and Delp, S. L., “Muscle contributions to propulsion and support during running,” *J. Biomech.*, vol. 43, no. 14, Oct. 2010, pp. 2709–2716.
- [81] Diaz, G. Y., Averett, D. H., and Soderberg, G. L., “Electromyographic analysis of selected lower extremity musculature in normal subjects during ambulation with and without a Protonics knee brace,” *J. Orthop. Sports Phys. Ther.*, vol. 26, no. 6, Dec. 1997, pp. 292–298.
- [82] Cerny, K., Perry, J., and Walker, J. M., “Effect of an unrestricted knee-ankle-foot orthosis on the stance phase of gait in healthy persons,” *Orthopedics*, vol. 13, no. 10, Oct. 1990, pp. 1121–1127.
- [83] Jansen, C. W., Olson, S. L., and Hasson, S. M., “The effect of use of a wrist orthosis during functional activities on surface electromyography of the wrist extensors in normal subjects,” *J. Hand Ther. Off. J. Am. Soc. Hand Ther.*, vol. 10, no. 4, Dec. 1997, pp. 283–289.
- [84] Bulthaup, S., Cipriani, D. J., and Thomas, J. J., “An electromyography study of wrist extension orthoses and upper-extremity function,” *Am. J. Occup. Ther. Off. Publ. Am. Occup. Ther. Assoc.*, vol. 53, no. 5, Oct. 1999, pp. 434–440.
- [85] Mattacola, C. G. and Dwyer, M. K., “Rehabilitation of the Ankle After Acute Sprain or Chronic Instability,” *J. Athl. Train.*, vol. 37, no. 4, 2002, pp. 413–429.

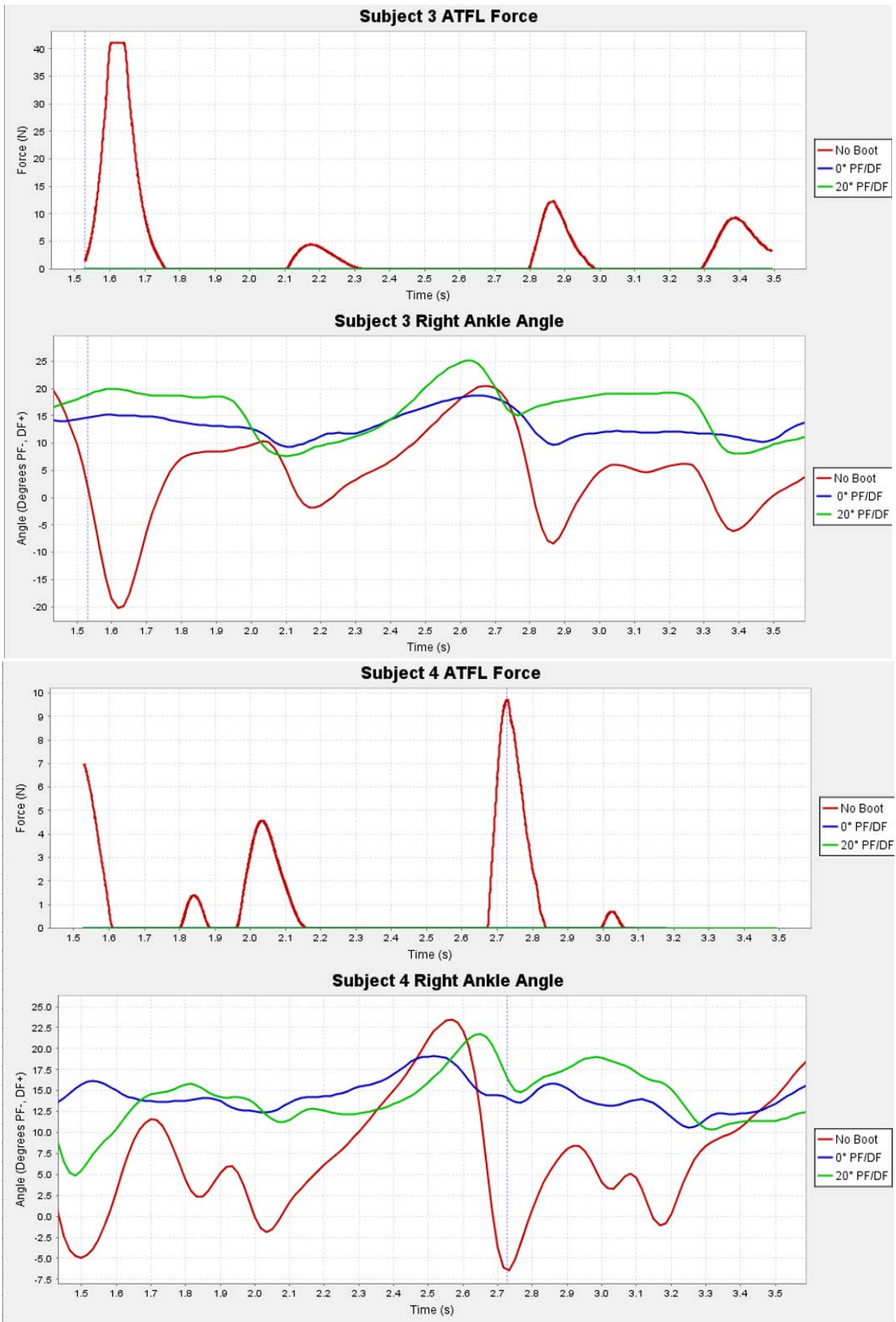
APPENDIXES

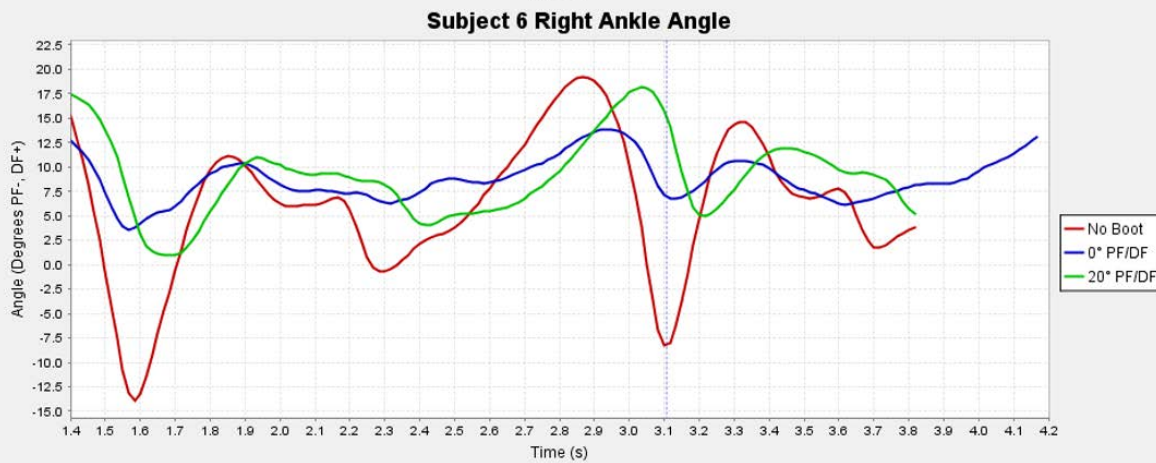
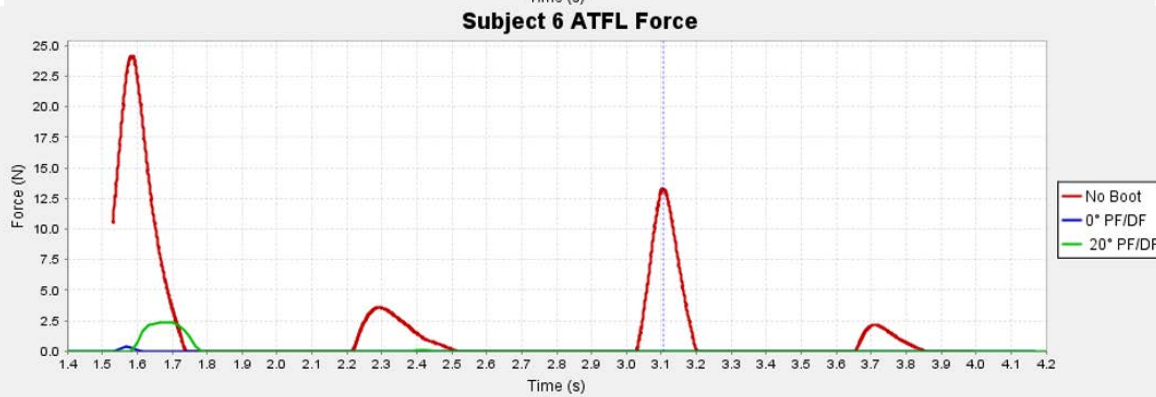
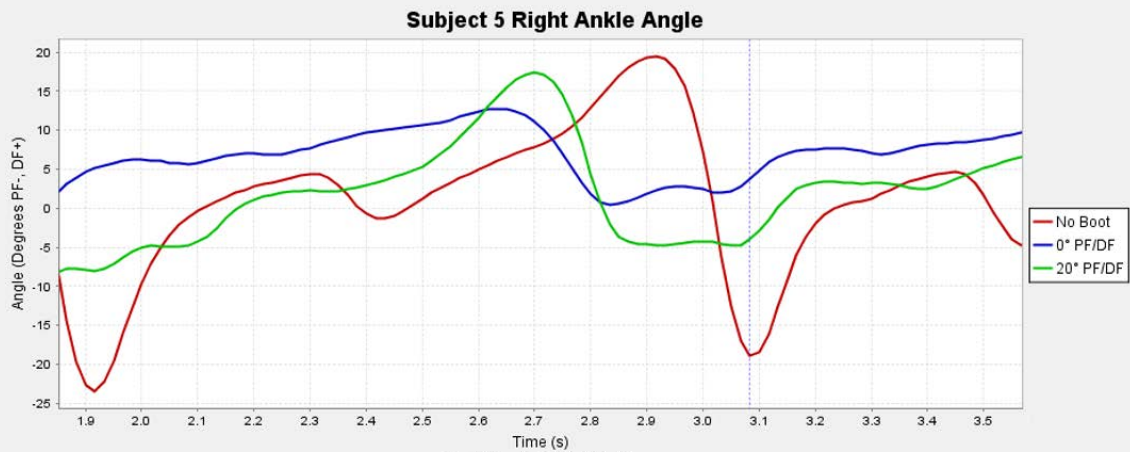
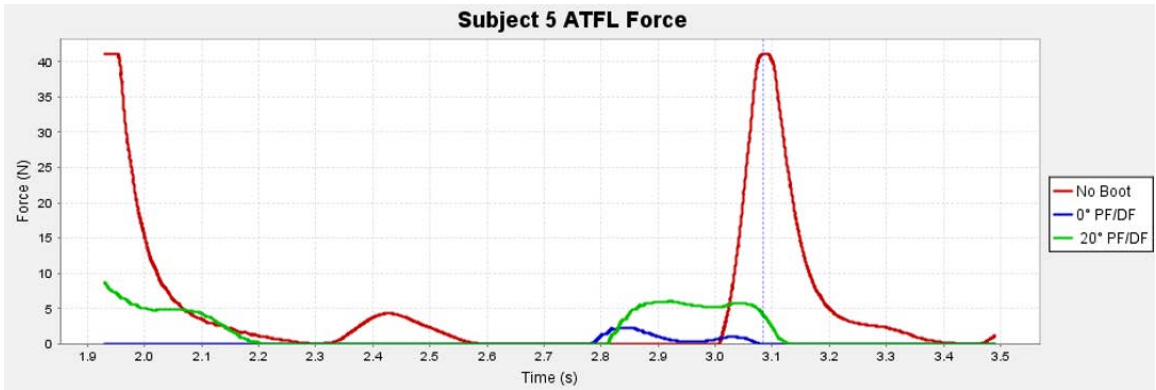
A Modified Gait Cycle

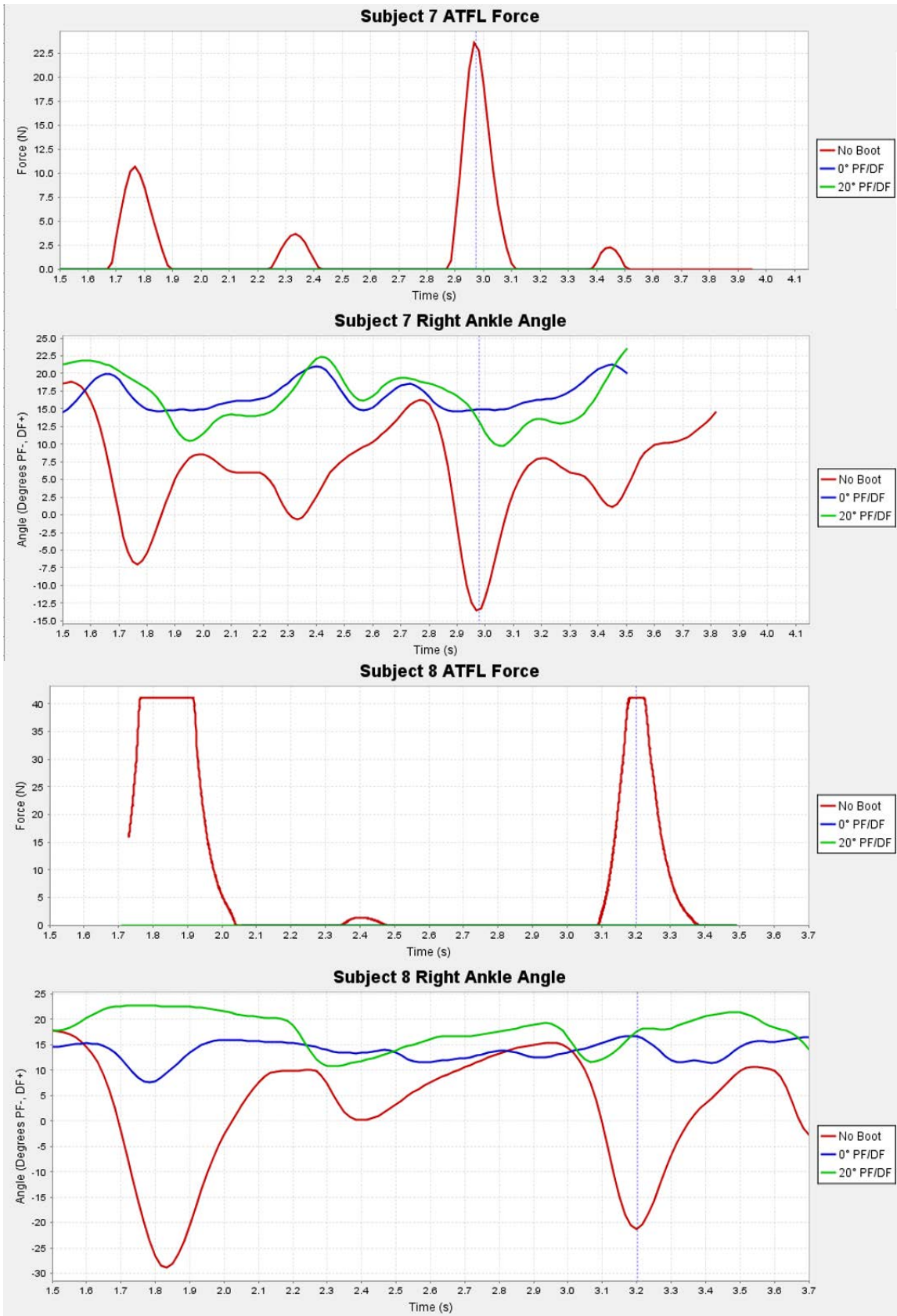


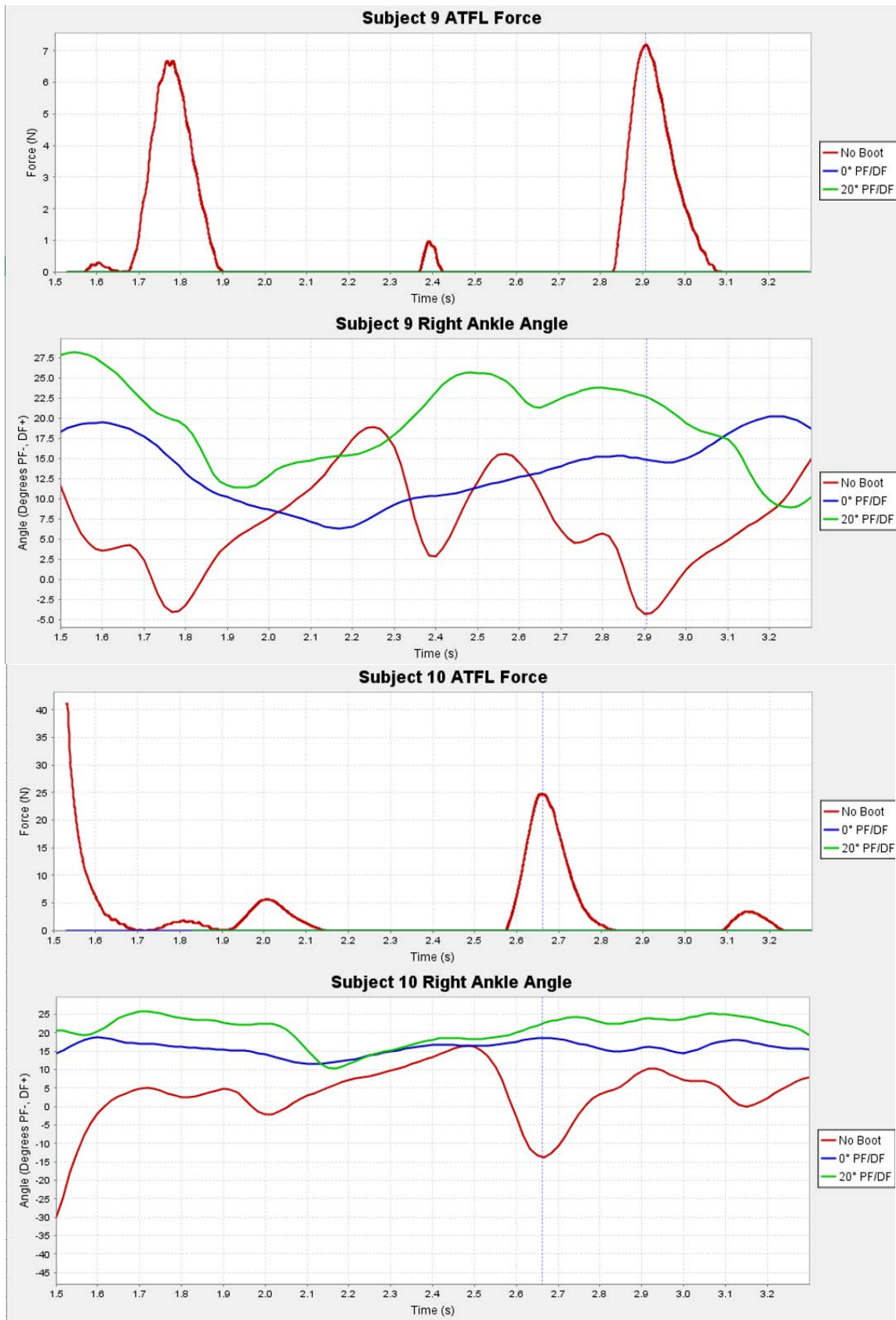
B Anterior Talofibular Ligament Forces and Ankle Joint Angles





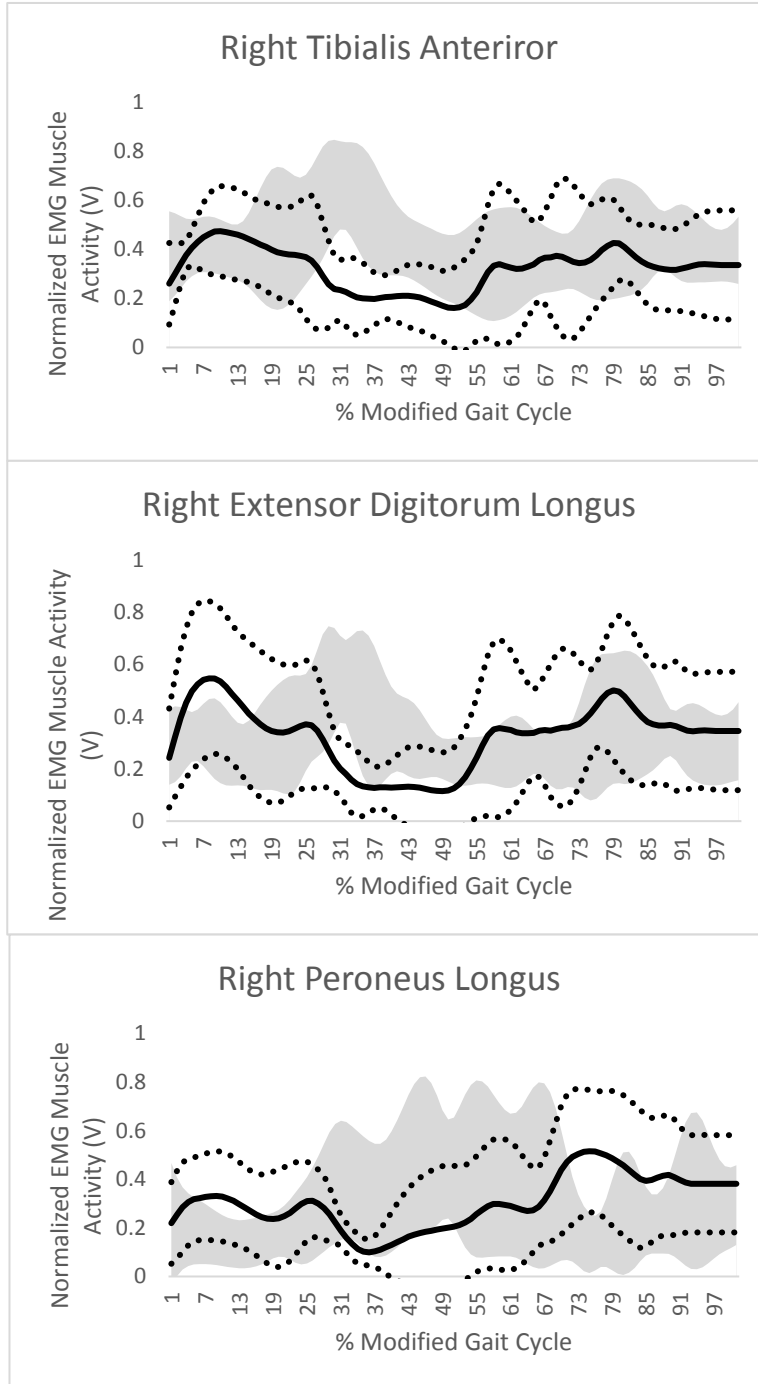






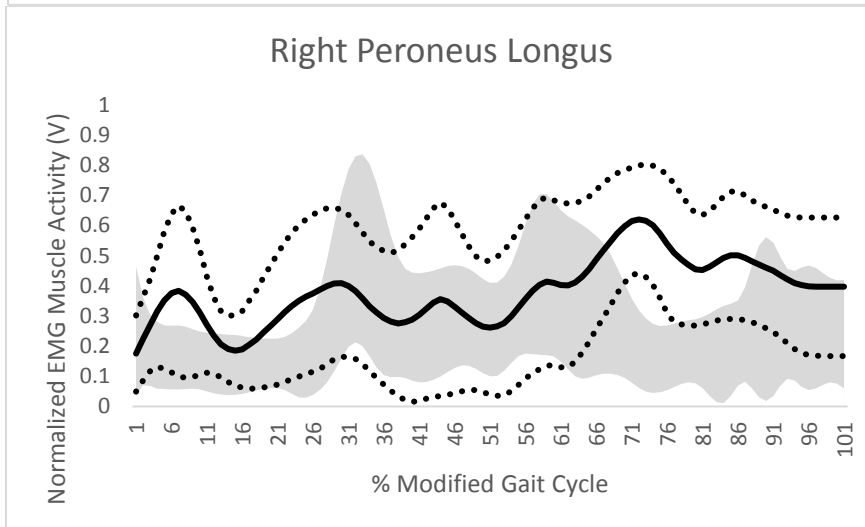
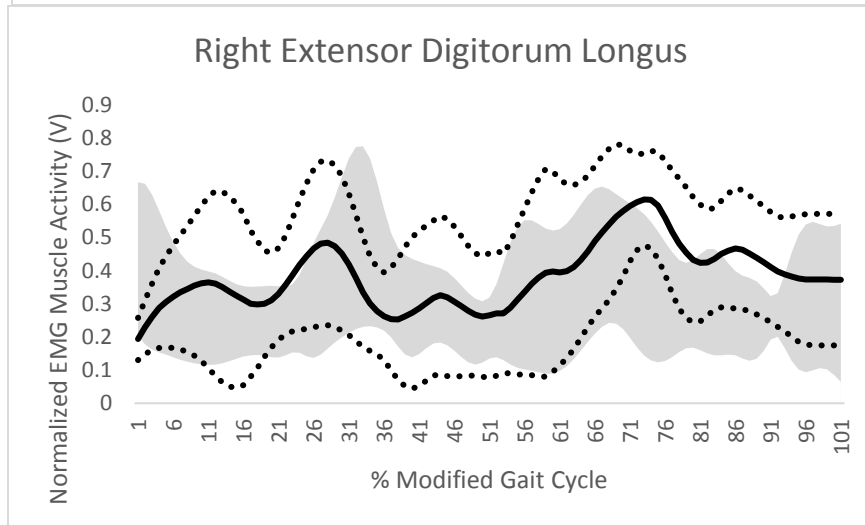
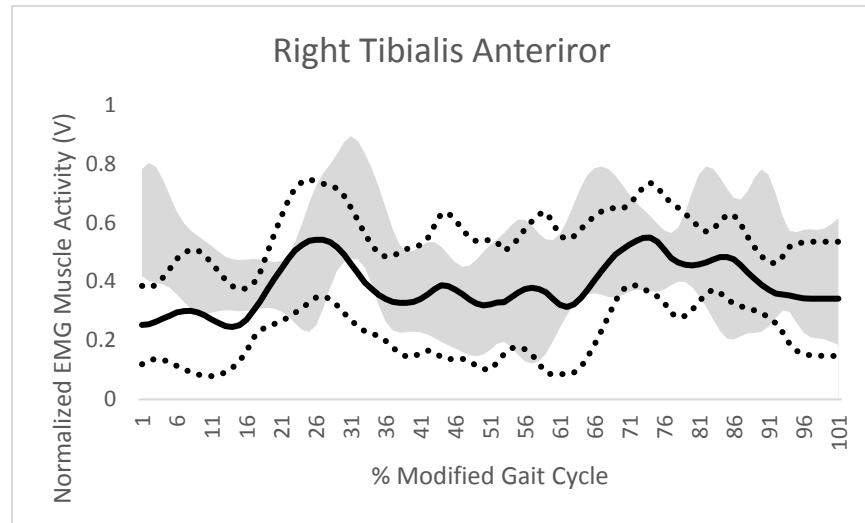
C Average Simulated Muscle Activations from Computed Muscle Control and Average Experimental EMG

NO BOOT CONDITION



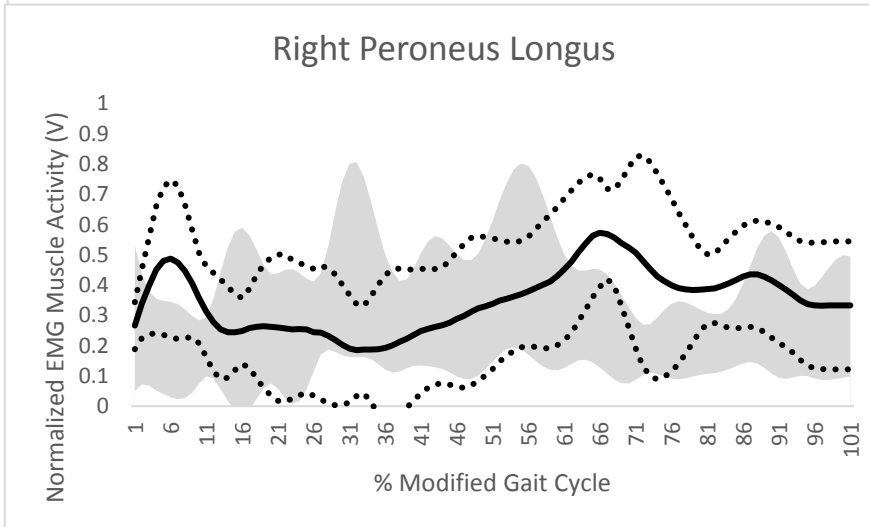
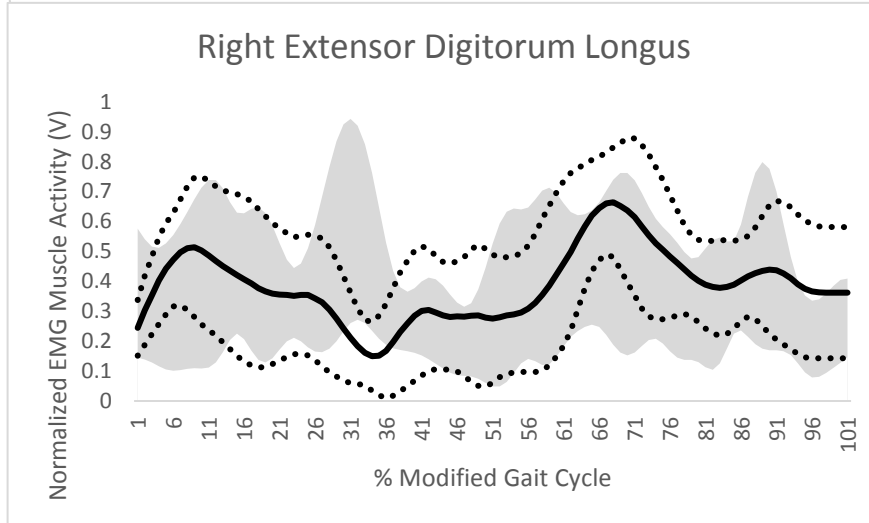
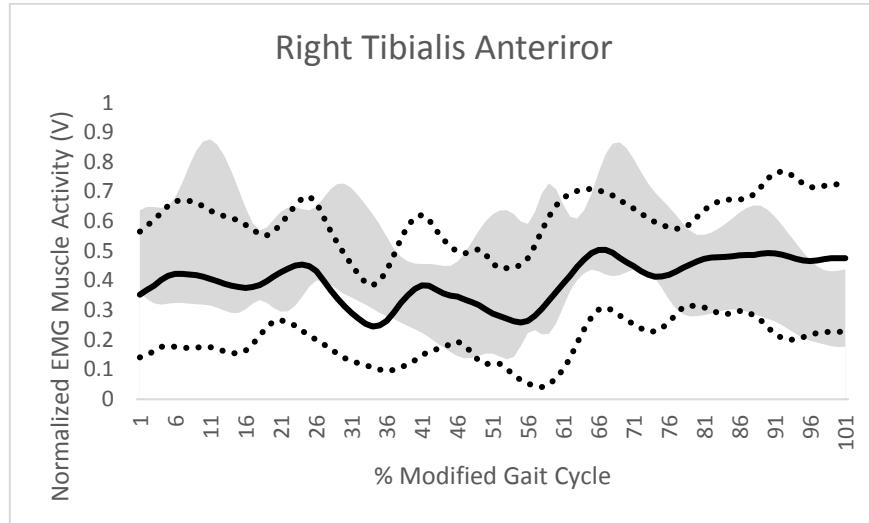
Average Experimental EMG
 Average OpenSim CMC Activity
 OpenSim \pm SD

0° PF/DF Condition



■ Average Experimental EMG — Average OpenSim CMC Activity OpenSim ±SD

20° PF/DF CONDITION



■ Average Experimental EMG — Average OpenSim CMC Activity OpenSim ±SD

D Statistical Analyses

Tibialis Anterior ANOVA

		Sum of Squares	df	Mean Square	F	Sig.
Mean	Between Groups	.10	5	.02	2.21	.071
	Within Groups	.39	42	.01		
	Total	.50	47			

Not Significantly Different
Not Significantly Different (Marginal)
Significantly Different

Tibialis Anterior LSD test

	(I) Condition	(J) Condition	Mean Difference (I - J)	Std. Error	<i>p</i> Sig.
LSD	No Boot EMG	Rigid EMG	-.04	.05	.467
		Articulated EMG	-.04	.05	.417
		No Boot OS	.10	.05	.050
		Rigid OS	.03	.05	.498
		Articulated OS	.02	.05	.680
	Rigid EMG	No Boot EMG	.04	.05	.467
		Articulated EMG	.00	.05	.933
		No Boot OS	.13	.05	.009
		Rigid OS	.07	.05	.164
		Articulated OS	.06	.05	.257
	Articulated EMG	No Boot EMG	.04	.05	.417
		Rigid EMG	.00	.05	.933
		No Boot OS	.14	.05	.007
		Rigid OS	.07	.05	.140
		Articulated OS	.06	.05	.224

Extensor Digitorum Longus ANOVA

		Sum of Squares	df	Mean Square	F	Sig.
Mean	Between Groups	.04	5	.01	1.00	.430
	Within Groups	.35	42	.01		
	Total	.40	47			

Not Significantly Different
Not Significantly Different (Marginal)
Significantly Different

Extensor Digitorum Longus LSD Test

	(I) Condition	(J) Condition	Mean Difference (I - J)	Std. Error	<i>p</i> Sig.
LSD	No Boot EMG	Rigid EMG	.01	.05	.910
		Articulated EMG	-.05	.05	.315
		No Boot OS	.00	.05	.950
	Rigid EMG	Rigid OS	-.06	.05	.190
		Articulated OS	-.06	.05	.171
		No Boot EMG	-.01	.05	.910
Articulated EMG	Articulated EMG	Articulated EMG	-.05	.05	.264
		No Boot OS	-.01	.05	.861
		Rigid OS	-.07	.05	.155
	Articulated OS	Articulated OS	-.07	.05	.139
		No Boot EMG	.05	.05	.315
		Rigid EMG	.05	.05	.264
		No Boot OS	.04	.05	.345
		Rigid OS	-.01	.05	.754
		Articulated OS	-.02	.05	.709

Peroneus Longus ANOVA

		Sum of Squares	df	Mean Square	F	Sig.
Mean	Between Groups	.13	5	.03	2.67	.035
	Within Groups	.41	42	.01		
	Total	.53	47			

Not Significantly Different
Not Significantly Different (Marginal)
Significantly Different

Peroneus Longus LSD Test

	(I) Condition	(J) Condition	Mean Difference (I - J)	Std. Error	<i>p</i> Sig.	
LSD	No Boot EMG	Rigid EMG	.04	.05	.410	
		Articulated EMG	.01	.05	.877	
		No Boot OS	-.02	.05	.619	
		Rigid OS	-.09	.05	.076	
		Articulated OS	-.10	.05	.043	
		Rigid EMG	No Boot EMG	-.04	.05	.410
		Articulated EMG	-.03	.05	.502	
		No Boot OS	-.07	.05	.189	
		Rigid OS	-.13	.05	.011	
		Articulated OS	-.14	.05	.006	
		Articulated EMG	No Boot EMG	-.01	.05	.877
		Rigid EMG	Rigid EMG	.03	.05	.502
		No Boot OS	-.03	.05	.515	
		Rigid OS	-.10	.05	.055	
		Articulated OS	Articulated OS	-.11	.05	.030

E Matlab Routine for Data Normalization

```
% start_EMGCMC_v1.m

clear all
clc

% Column 1 is time
EMGcol = [1, 2, 3, 4];
OSimcol = [1, 122, 130, 126];

froot1 = 'C:\Users\Biomech\Desktop\Pedro ANC vs STO'; %C:\CMC simulation\';

froot2 = 'C:\Users\Biomech\Desktop\Pedro ANC vs STO\Start_End';

% no_EMGfiles = dir([froot1, '**_no_EMG.anc']);
%
% no_OSimfiles = dir([froot1, '**_no_states.sto'])
%
% 0_EMGfiles = dir([froot1, '**_0_EMG.anc']);
%
% 0_Osimfiles = dir([froot1, '**_0_states.sto'])
%
% 20_EMGfiles = dir([froot1, '**_20_EMG.anc']);
%
% 20_OSimfiles = dir([froot1, '**_20_states.sto']);
%
%% Filtering
% sample frequency Hz
samplfreqEMG = 1500;
samplefreqOSim = 4000;
% cutoff freq Hz
cutoff = 6;
% Nyquist freq
WnEMG = samplfreqEMG/2;
WnOSim = samplefreqOSim/2;
% Generate filter coefficients
[B, A] = butter(6, cutoff/WnEMG);
[C, D] = butter(6, cutoff/WnOSim);

% Read walking start and end for three conditions
start_end = xlsread('walking_subj_start_end_time');

%% Note: there is no \Subject 6 & 7, so skip this number
subjnum = [1 2 3 4 5 8 9 10];

% create counter
count = 1;
for IT1 = subjnum
    %no boot rectify, filter, and with time column
    no_EMGdata = []; no_EMGraw = [];
    no_EMGdata = dlmread([froot1 '\Subject' int2str(IT1)
'_no_EMG.anc'], '\t', 11, 0);
    no_EMGraw = abs(no_EMGdata(:, EMGcol(2:end)));
    no_EMG = filtfilt(B, A, no_EMGraw);
end
```

```

no_EMGwithtime = [ no_EMGdata(:,EMGcol(1)),no_EMG];

no_OSimdata = []; no_OSimraw =[];
no_OSimdata = dlmread([froot1 '\Subject' int2str(IT1)
'_no_states.sto'], '\t', 7, 0);
no_OSimraw = abs(no_OSimdata(:,OSimcol(2:end)));
no_OSim= filtfilt(C, D, no_OSimraw);
no_OSimwithtime = [ no_OSimdata(:,OSimcol(1)),no_OSim];

Z_EMGdata = []; Z_EMGraw =[];
Z_EMGdata = dlmread([froot1 '\Subject' int2str(IT1)
'_0_EMG.anc'], '\t', 11, 0);
Z_EMGraw = abs(Z_EMGdata(:,EMGcol(2:end)));
Z_EMG = filtfilt(B, A, Z_EMGraw);
Z_EMGwithtime = [ Z_EMGdata(:,EMGcol(1)),Z_EMG];

Z_OSimdata = []; Z_OSimraw =[];
Z_OSimdata = dlmread([froot1 '\Subject' int2str(IT1)
'_0_states.sto'], '\t', 7, 0);
Z_OSimraw = abs(Z_OSimdata(:,OSimcol(2:end)));
Z_OSim = filtfilt(C, D, Z_OSimraw);
Z_OSimwithtime = [ Z_OSimdata(:,OSimcol(1)),Z_OSim];

T_EMGdata = []; T_EMGraw =[];
T_EMGdata = dlmread([froot1 '\Subject' int2str(IT1)
'_20_EMG.anc'], '\t', 11, 0);
T_EMGraw = abs(T_EMGdata(:,EMGcol(2:end)));
T_EMG = filtfilt(B, A, T_EMGraw);
T_EMGwithtime = [ T_EMGdata(:,EMGcol(1)),T_EMG];

T_OSimdata = []; T_OSimraw =[];
T_OSimdata = dlmread([froot1 '\Subject' int2str(IT1)
'_20_states.sto'], '\t', 7, 0);
T_OSimraw = abs(T_OSimdata(:,OSimcol(2:end)));
T_OSim = filtfilt(C, D, T_OSimraw);
T_OSimwithtime = [ T_OSimdata(:,OSimcol(1)),T_OSim];

%start and end time file
time = start_end(1,6*IT1-5:6*IT1);

%define start and end time
tstartnoEMG = min(find(no_EMGwithtime(:,1) >= time(1,1)));
tstartnoOSim = min(find(no_OSimwithtime(:,1) >= time(1,1)));
tendnoEMG = min(find(no_EMGwithtime(:,1) >= time(1,2)));
tendnoOSim = min(find(no_OSimwithtime(:,1) >= time(1,2)));
tstartZEMG = min(find(Z_EMGwithtime(:,1) >= time(1,3)));
tstartZOSim = min(find(Z_OSimwithtime(:,1) >= time(1,3)));
tendZEMG = min(find(Z_EMGwithtime(:,1) >= time(1,4)));
tendZOSim = min(find(Z_OSimwithtime(:,1) >= time(1,4)));
tstartTEMG = min(find(T_EMGwithtime(:,1) >= time(1,5)));
tstartTOSim = min(find(T_OSimwithtime(:,1) >= time(1,5)));

```

```

tendTEMG = min(find(T_EMGwithtime(:,1) >= time(1,6)));
tendTOSim = min(find(T_OSimwithtime(:,1) >= time(1,6)));

%input start and end time and store files
noEMG1 = no_EMGwithtime(tstartnoEMG:tendnoEMG,:);

noOSim1 = no_OSimwithtime(tstartnoOSim:tendnoOSim,:) ;
noOSimall (count).data = [noOSim1];
noOSimall (count).name = ['\Subject', int2str(IT1), '_no_states.sto'];

ZEMG1 = Z_EMGwithtime(tstartZEMG:tendZEMG,:);

ZOSim1 = Z_OSimwithtime(tstartZOSim:tendZOSim,:) ;
ZOSimall (count).data = [ZOSim1];
ZOSimall (count).name = ['\Subject', int2str(IT1), '_0_states.sto'];

TEMG1 = T_EMGwithtime(tstartTEMG:tendTEMG,:);

TOSim1 = T_OSimwithtime(tstartTOSim:tendTOSim,:) ;
TOSimall (count).data = [TOSim1];
TOSimall (count).name = ['\Subject', int2str(IT1), '_20_states.sto'];

a(1,:) = max (noEMG1(:,2:end));
a(2,:) = max (ZEMG1(:,2:end));
a(3,:) = max (TEMG1(:,2:end));
EMGmax1 = max (a);
EMGmax = [1 EMGmax1];

noEMGnorm = bsxfun(@rdivide,noEMG1, EMGmax);
noEMGall (count).data = [noEMGnorm];
noEMGall (count).name = ['\Subject', int2str(IT1), '_no_EMG.anc'];

ZEMGnorm = bsxfun(@rdivide,ZEMG1, EMGmax);
ZEMGall (count).data = [ZEMGnorm];
ZEMGall (count).name = ['\Subject', int2str(IT1), '_0_EMG.anc'];

TEMGnorm = bsxfun(@rdivide,TEMG1, EMGmax);
TEMGall (count).data = [TEMGnorm];
TEMGall (count).name = ['\Subject', int2str(IT1), '_20_EMG.anc'];
count = count + 1;
end

%interpolation%
count1 = 1;
for IT2 =1:8
    t= noEMGall(IT2).data(:,:);
    x= t(1,1):(t(end,1)-t(1,1))/100:t(end,1);
    y=interp1(t(:,1),t(:,2:end),x);
    noEMGallinter (count1).data = y;
    noEMGallinter (count1).name = ['\Subject', int2str(IT1), '_no_EMG.anc'];

    t1= noOSimall(IT2).data (:,:);
    x1= t1(1,1):(t1(end,1)-t1(1,1))/100:t1(end,1);

```

```

y1=interp1(t1(:,1),t1(:,2:end),x1);
noOSimallinter (count1).data = y1;
noOSimallinter (count1).name = ['\Subject', int2str(IT1),
'_no_states.sto'];

t2= ZEMGall(IT2).data(:,:);
x2= t2(1,1):(t2(end,1)-t2(1,1))/100:t2(end,1);
y2=interp1(t2(:,1),t2(:,2:end),x2);
ZEMGallinter (count1).data = y2;
ZEMGallinter (count1).name = ['\Subject', int2str(IT1), '_0_EMG.anc'];

t3= ZOSimall(IT2).data(:,:);
x3= t3(1,1):(t3(end,1)-t3(1,1))/100:t3(end,1);
y3=interp1(t3(:,1),t3(:,2:end),x3);
ZOSimallinter (count1).data = y3;
ZOSimallinter (count1).name = ['\Subject', int2str(IT1),
'_0_states.sto'];

t4= TEMGall(IT2).data(:,:);
x4= t4(1,1):(t4(end,1)-t4(1,1))/100:t4(end,1);
y4=interp1(t4(:,1),t4(:,2:end),x4);
TEMGallinter (count1).data = y4;
TEMGallinter (count1).name = ['\Subject', int2str(IT1), '_20_EMG.anc'];

t5= TOSimall(IT2).data(:,:);
x5= t5(1,1):(t5(end,1)-t5(1,1))/100:t5(end,1);
y5=interp1(t5(:,1),t5(:,2:end),x5);
TOSimallinter (count1).data = y5;
TOSimallinter (count1).name = ['\Subject', int2str(IT1),
'_20_states.sto'];

count1 = count1+1;
end

xaxislimits = [0 100];
for IT3 = 1:8

figure;
subplot (3,3,1);
plot (noOSimallinter(IT3).data(:,1));
hold on
plot (noEMGallinter(IT3).data(:,1), 'r');
title ('Tib Ant');
xlim(xaxislimits);

subplot (3,3,2);
plot (noOSimallinter(IT3).data(:,2));
hold on
plot (noEMGallinter(IT3).data(:,2), 'r');
title ('Ext Dig');
xlim(xaxislimits);

subplot (3,3,3);
plot (noOSimallinter(IT3).data(:,3));
hold on

```

```

plot (noEMGallinter(IT3).data(:,3), 'r');
title ('Per Long');
legend('noOSim','noEMG');
xlim(xaxislimits);

% figure;
subplot (3,3,4);
plot (ZOSimallinter(IT3).data(:,1));
hold on
plot (ZEMGallinter(IT3).data(:,1), 'r');
title ('Tib Ant');
xlim(xaxislimits);

subplot (3,3,5);
plot (ZOSimallinter(IT3).data(:,2));
hold on
plot (ZEMGallinter(IT3).data(:,2), 'r');
title ('Ext Dig');
xlim(xaxislimits);

subplot (3,3,6);
plot (ZOSimallinter(IT3).data(:,3));
hold on
plot (ZEMGallinter(IT3).data(:,3), 'r');
xlim(xaxislimits);
title ('Per Long');
legend ('0\_OSim', '0\_EMG');

%figure;
subplot (3,3,7);
plot (TOSimallinter(IT3).data(:,1));
hold on
plot (TEMGallinter(IT3).data(:,1), 'r');
xlim(xaxislimits);
title ('Tib Ant');

subplot (3,3,8);
plot (TOSimallinter(IT3).data(:,2));
hold on
plot (TEMGallinter(IT3).data(:,2), 'r');
xlim(xaxislimits);
title ('Ext Dig');

subplot (3,3,9);
plot (TOSimallinter(IT3).data(:,3));
hold on
plot (noEMGallinter(IT3).data(:,3), 'r');
xlim(xaxislimits);
title ('Per Long');
legend('20\_OSim', '20\_EMG');

end

```

F Opensim Ligament Class

```
<Ligament name="TaloFibularAnt_r">
  <!--the set of points defining the path of the ligament-->
  <GeometryPath>
    <!--The set of points defining the path-->
    <PathPointSet>
      <objects>
        <PathPoint name="TaloFibularAnt_r_P1">
          <location> 0.00482732 -0.405495 0.0251021</location>
          <body>tibia_r</body>
        </PathPoint>
        <PathPoint name="TaloFibularAnt_r_P2">
          <location> 0.0241366 -0.00289639 0.00579278</location>
          <body>talus_r</body>
        </PathPoint>
      </objects>
      <groups />
    </PathPointSet>
    <!--Used to display the path in the 3D window-->
    <VisibleObject name="display">
      <!--Set of geometry files and associated attributes, allow
.vtp, .stl, .obj-->
      <GeometrySet>
        <objects />
        <groups />
      </GeometrySet>
      <!--Three scale factors for display purposes: scaleX scaleY
scaleZ-->
      <scale_factors> 1 1 1</scale_factors>
      <!--transform relative to owner specified as 3 rotations (rad)
followed by 3 translations rX rY rZ tx ty tz-->
      <transform> -0 0 -0 0 0 0</transform>
      <!--Whether to show a coordinate frame-->
      <show_axes>>false</show_axes>
      <!--Display Pref. 0:Hide 1:Wire 3:Flat 4:Shaded Can be
overriden for individual geometries-->
      <display_preference>1</display_preference>
    </VisibleObject>
    <!--Used to initialize the colour cache variable-->
    <default_color>0.9 0.9 0.9</default_color>
  </GeometryPath>
  <!--resting length of the ligament-->
  <resting_length>0.0291215084286951</resting_length>
  <!--force magnitude that scales the force-length curve-->
  <pcsa_force>47.5276365762363</pcsa_force>
  <!--Function representing the force-length behavior of the
ligament-->
  <SimmSpline name="force_length_curve">
    <x> -5 0.998 0.999 1 1.015 1.03 1.045 1.06 1.075 1.09 1.105 1.12
1.135 1.15 1.165 1.166 1.166 5</x>
    <y> 0 0 0 0 0.0279035 0.0604477 0.0984197 0.143131 0.196418
0.260642 0.338688 0.433967 0.550413 0.692486 0.865171 0.865171 0.865171
0.865171</y>
  </SimmSpline>
</Ligament>
```